PALÆO VERTEBRATA

MONOGRAPH

Comparative bone histology of rhabdodontid dinosaurs

EDINA PRONDVAI

MTA-ELTE Lendület Dinosaur Research Group, Pázmány Péter sétány 1/c, Budapest, 1117, Hungary
E-mail: edina.prondvai@gmail.com

Abstract: A comparative bone histological study of the three known genera of the endemic European ornithopod dinosaur family, Rhabdodontidae, is presented here in an ontogenetic context. Investigated specimens were assigned to different ontogenetic stages based exclusively on the histological indicators of osteologic maturation during diametrical bone growth; an entirely size-independent method as opposed to most previous studies. Qualitative comparison of bone histology of corresponding ontogenetic stages and elements among the three valid rhabdodontid genera, *Mochlodon*, *Zalmoxes*, and *Rhabdodon*, revealed some consistent patterns. Genus specific histological differences within Rhabdodontidae are most expressed between *Rhabdodon* and the *Mochlodon-Zalmoxes* clade. These indicate a prolonged phase of fast growth and a less constrained cyclicity in the growth dynamics of *Rhabdodon*, as opposed to the slower and more regulated growth strategy reflected in the bones of *Mochlodon* and *Zalmoxes*. These genus specific differences are consistent with the phylogenetic interrelation of the genera and are most probably related to the pronounced differences in body size. However, when compared to other ornithopods, most detected histological features in rhabdodontids do not seem to reliably reflect either phylogenetic relations or body size. A notable common feature of all rhabdodontid genera irrespective of body size is the ontogenetically early onset of cyclical growth and secondary remodelling; a pattern that more resembles the condition found in derived ornithopods than that described in more basal taxa which are closer relatives of rhabdodontids. The recognition of taxon-specific histological patterns as well as patterns indicative of ecological and thereby functional traits clearly requires more accurate, preferably quantitative evaluations.

Keywords: bone histology-based ontogeny, *Mochlodon*, *Rhabdodon*, skeletal maturation, *Zalmoxes*

Submitted 19 June 2014, Accepted 1 October 2014

INTRODUCTION

The phylogeny and some paleobiological aspects of the endemic European Late Cretaceous family of ornithopod dinosaurs, the Rhabdodontidae Weishampel, Jianu, Csiki, et Norman, 2003 have recently been in the focus of a thorough investigation (Ősi *et al*. 2012). Although the latter study extensively used bone histology to infer body size evolution in this ornithopod group, the authors only presented information necessary to conclude on the relative ontogenetic stages of the examined specimens in order to assess their adult sizes. Since bone histology of other ornithopod dinosaurs has been profoundly investigated by a number of studies with respect to different aspects of growth dynamics (Chinsamy, 1995; Chinsamy *et al*. 1998; Horner *et al*. 2000, 2009; Woodward *et al*. 2011; Hübner, 2012; Werning, 2012), these studies represent a comprehensive framework into which histological data of the available rhabdodontid material can fruitfully be inserted. Thus, current work represents the follow up study of Ősi *et al*. (2012), and aims to give a detailed qualitative description of the bone microstructure of each specimen acquired in the previous study, thereby providing basic histological information of each genus of Rhabdodontidae recognized so far. These three valid genera are the type genus *Rhabdodon* Matheron, 1869 known from France (e.g., Buffetaut *et al*. 1993; Allain & Pereda Superbiola, 2003) and Spain (Pereda Superbiola & Sanz, 1999; Company, 2004), *Zalmoxes* Weishampel, Jianu, Csiki, et Norman, 2003 described from what is now Romania (e.g., Nopcsa, 1902; Godfroit *et al*. 2009; Benton *et al*. 2010), and *Mochlodon* Seeley, 1881, the recently resurrected genus found in Austria (Bunzel, 1871) and Hungary (Ősi *et al*. 2012). Taxonomic and phylogenetic context of this study relies on previous work (Ősi *et al*. 2012, Benton *et al*. 2010) that identified two species of *Mochlodon* (*M. suessi* Seeley, 1881 and *M. vorosi* Ősi, Prondvai, Butler, et Weishampel, 2012) and *Zalmoxes* (*Z. robustus* and *Z. shqiperorum* Weishampel, Jianu, Csiki, et Norman, 2003) in the current sample, whereas no species was assigned to the sampled specimens of *Rhabdodon*. An exclusively histology based ontogenetic classification approach is also introduced here in detail and applied to assign a relative developmental stage to the sampled rhabdodontid specimens. The qualitative comparison of the histological characteristics of rhabdodontids with those of other ornithopods enables us to seek consistent microstructural patterns that may be of taxonomic, ecological and/or functional importance.

Institutional abbreviations: FGGUB, Facultatea de Geologie şi Geofizică, Universitatea Bucureşti, Bucharest, Romania; IPB, Steinmann Institute for Geology, Mineralogy andPaleontology, University of Bonn, Bonn, Germany; MC, Mechin Collection (private collection), Vitrolles, France; MHN, Muséum d'Histoire Naturelle d'Aix-en-Provence, Aix-en-Provence, France; MTM, Hungarian Natural History Museum, Budapest, Hungary; PIUW, Paleontology Institute, University of Vienna, Vienna, Austria.

Abbreviations in the Figures:

an, annulus
cccb, compacted coarse cancellous bone
cmc, crushed medullary cavity
cn, canaliculi

csr, complete secondary remodelling
dml, diagenetically modified lacunae
DO-l, dynamic osteogenesis-derived lacunae
ec, erosion cavities
EFS, external fundamental system
eic, eroded inner cortex
el, endosteal lamellae
eps, eroded periosteal surface
gc, growth cycles
LAG, line of arrested growth
lfb, longitudinal structural fibres
mc, medullary cavity
oEFS, onset of EFS
pb, primary bone
"pp", posterolateral plug
prl, periosteal resorption line
ps, periosteal surface
pvc, primary vascular canals
Shf, Sharpey's fibres
so, secondary osteons
SO-l, static osteogenesis-derived lacunae
sr, secondary remodeling
st, diagenetic staining
wb, woven bone

MATERIALS AND METHODS

The examined material is identical to the specimens sampled for the study of Ősi *et al*. (2012, and see Table 1). However, in addition to the transverse sections already available, longitudinal sections of each core sample of *Rhabdodon* specimens were also prepared following standard methods (e.g., Wells, 1989). Thin sections prepared in transverse as well as longitudinal section planes provide us with more reliable information concerning the three-dimensional structure of the bone tissue (see Stein & Prondvai, 2014; Prondvai *et al*. 2014a). The relatively high number of sampled specimens in the genus *Rhabdodon* with sometimes multiple core samples of the same element offers good opportunity to check histovariability not only among different specimens but also along the long axis of the bone. Although thin sections of *Zalmoxes* used in this study were prepared and already published by Benton *et al*. (2010), some important details, such as sampling location and sampling method were not reported in their work. For further details about the sectioned specimens, see Table 1.

All sections were investigated under Nikon LV 100 polarized light microscope (Nikon Corp., Tokyo, Japan). Birefringence properties were observed under crossed plane polarizers without as well as with the aid of a λ wave plate that enhances visibility of some microstructural features and improves image quality. Pictures were acquired with a QImaging MP5.0 digital microscope camera (QImaging Corp., Surrey BC., Canada) and processed with Image Pro Insight 8.0 (Media Cybernetics L.P., Maryland, USA) software. All figures present in this study were constructed using CorelDRAW X5 (Corel Corp., Ottawa, Canada) software.

Tissue identification concept and terminology used in the histological descriptions mainly follows Stein & Prondvai (2014) and Prondvai *et al*. (2014a) with some fundamental terms adopted from Francillon-Vieillot *et al*. (1990) and Marotti (2010). The reference axis according to which directions of cutting planes and orientation of microstructures are given is the longitudinal axis of the bone.

Although the ontogenetic stages and inferred body sizes of all of these specimens have been defined by Ősi *et al*. (2012), in the light of the modified paleohistological concept discussing methods of tissue identification and interpretation introduced by Stein & Prondvai (2014) and Prondvai *et al*. (2014a), a revision of the bone microstructure including the ontogenetic assignment of each specimen is provided here. Unfortunately, the available sampled bones do not always represent the same skeletal elements, and because of their preservational and/or scientific value there are differences in relative sampling locations as well as in sampling techniques. Consequently, quantitative measurements of histological characters in order to assign relative ontogenetic stages to specimens (as in Prondvai *et al*. 2014b) were not reasonable. Thus, developmental status of each specimen was identified based exclusively on a size-independent, qualitative histological evaluation of the thin sections. For this purpose, size independent relative ontogenetic categories were established, such as early and late juveniles, subadults and adults. Juveniles are defined as exhibiting no histological indication of a substantial slow-down of growth towards the outermost cortex but rather as showing continuous or cyclical growth where the successive thick zones were seemingly deposited at similar, random, or slightly decreasing rates. Early and late juveniles are distinguished based on the combination of the following characters: 1) change in relative zone thickness towards bone periphery; 2) relative degree of compaction of primary cavities, i.e., primary cortical porosity; 3) number of growth marks; 4) extent and architecture of secondary remodelling; 5) proportional amount of woven bone derived from static osteogenesis (SO, see Marotti, 2010; Stein & Prondvai, 2014; Prondvai *et al*. 2014a) in the outer cortex. In early juveniles we expect that zone thickness does not tend to progressively decrease towards the outer cortex, whereas in late juveniles there may be a trend of slightly decreasing zone-width peripherally. Furthermore, in early juveniles the primary canals are much less compacted resulting in a sensibly higher cortical porosity, the number of growth marks is less, secondary remodelling affects a lower proportion of the cortex, and the proportional amount of woven bone is higher than in late juveniles. Subadults are expected to show microstructural evidence of a substantial decrease in bone growth rate such as considerably decreasing vascularity and width of zones between growth marks towards the periosteal surface, low porosity, vascular architecture with less transverse anastomoses in the outer cortical regions, and occasionally more extensive secondary remodelling. Adult state is defined if histology suggests complete cessation of bone growth by showing the development of an external fundamental system (EFS, Cormack, 1987) with closely packed lines of arrested growth (LAGs) in the almost avascular outermost cortex (Horner *et al*. 1999) or complete cortical remodelling (see Stein *et al*. 2010). This gradual transition of different histological characters from early juveniles up to adults describes the general pattern of growth and maturation of bone tissues (e.g., Enlow, 1962; Chinsamy, 1993; Varricchio, 1993; Curry, 1999; Erickson & Tumanova, 2000; Horner *et al*. 2000, 2009; Chinsamy-Turan, 2005; Erickson, 2005; Klein & Sander, 2008). The expected direction of change in the considered osteohistological features in relation to skeletal maturation is demonstrated in Figure 1A. Nonetheless, variance in these features is also expected, i.e., one characteristic not following the expected pattern does not exclude the specimen from being assigned to a category that most other histological features correspond with.

Although these histologic definitions of ontogenetic stage

Species/ genus	Specimen ID	Fig. code	Sampled element	Sampling location	Sampling method	Element length (mm; *estimated)	Histology-based ontogenetic stage
Mochlodon vorosi	MTM 2012.25.1	1	?right femur	mid-diaphysis	complete transverse section	217	late juvenile
	MTM 2012.26.1	2	right tibia	distal diaphysis	complete transverse section	179*	late juvenile
	MTM V 2010.126.1	3	left femur	anterior side; mid-diaphysis	broken off piece of outer cortex	160*	subadult
	MTM V 01.101	4	?right tibia	?medial side; mid-diaphysis	broken off piece of outer cortex	148*	subadult
	MTM 2012.23.1	5	left humerus	mid-diaphysis	complete transverse section	156	adult
	MTM V 01.225	6	left femur	lateral side; mid-diaphysis	broken off piece of outer cortex	218*	adult
Mochlodon suessi	PIUW 3518	7	left scapula	mid-shaft	complete transverse section	162*	early juvenile
	PIUW 3517	8	?radius	mid-diaphysis	complete transverse section	82*	early juvenile
	PIUW 2349/III	9	left femur	proximal diaphysis	complete transverse section	105*	early juvenile
	PIUW 2349/35	10	right tibia	mid-diaphysis	half transverse section	181*	adult
Zalmoxes robustus	FGGUB R.1392	11	right humerus	?	?	201*	late juvenile
	FGGUB R.1382	12	left femur	?	?	280*	late juvenile - subadult
	FGGUB R.1002	13	left femur	?	?	320*	subadult
Zalmoxes shqiperorum	FGGUB R.1088	14	left femur	?	?	164*	early juvenile
	FGGUB R.1608	15	left femur	?	?	333	subadult
Zalmoxes sp.	FGGUB OB 3077	16	left humerus	?	?	255	late juvenile
	FGGUB R.6	17	right humerus	?	?	180*	subadult
Rhabdodon sp.	MHN AIX PV 2001.12.294	18	right humerus	anterior side; mid-diaphysis	core drilling	236	early juvenile
	MHN AIX PV 2001.65	19	left humerus	anterior side; mid- diaphysis	core drilling	298	early juvenile
	MHN AIX PV 1999.12	20	right humerus	anterior side; distal diaphysis	core drilling	352*	late juvenile
	MHN AIX PV 2001.113	21	left femur	anterior side; proximal diaphysis	core drilling	718*	late juvenile
	MHN AIX PV 2001.A3	22	left femur	anterior side; mid-diaphysis	core drilling	626*	late juvenile
	MC 472	23	left humerus	posterior side; mid-diaphysis	core drilling	326*	late juvenile
	MC 676	24	right femur	anterior side; mid-diaphysis	core drilling	703*	late juvenile
	MHN AIX PV 2001.27	25	right femur	anterior side; mid-diaphysis & proximal metaphysis	core drilling	513*	late juvenile - subadult
	MHN AIX PV 2007.4.115	26	?right femur	?anterior side; mid-diaphysis & distal metaphysis	core drilling	688*	subadult
	MHN AIX PV 2007.4.116	27	right femur	?anterior side; mid-diaphysis, proximal & distal metaphysis	core drilling	820*	adult
	MHN AIX PV 2008.1.11	28	right femur	anterior side; mid-diaphysis	core drilling	210	adult

Table 1. Details of the sampled specimens. Question marks in the sampling location and sampling method columns for *Zalmoxes* indicate that these data were not reported by Benton *et al*. (2010).

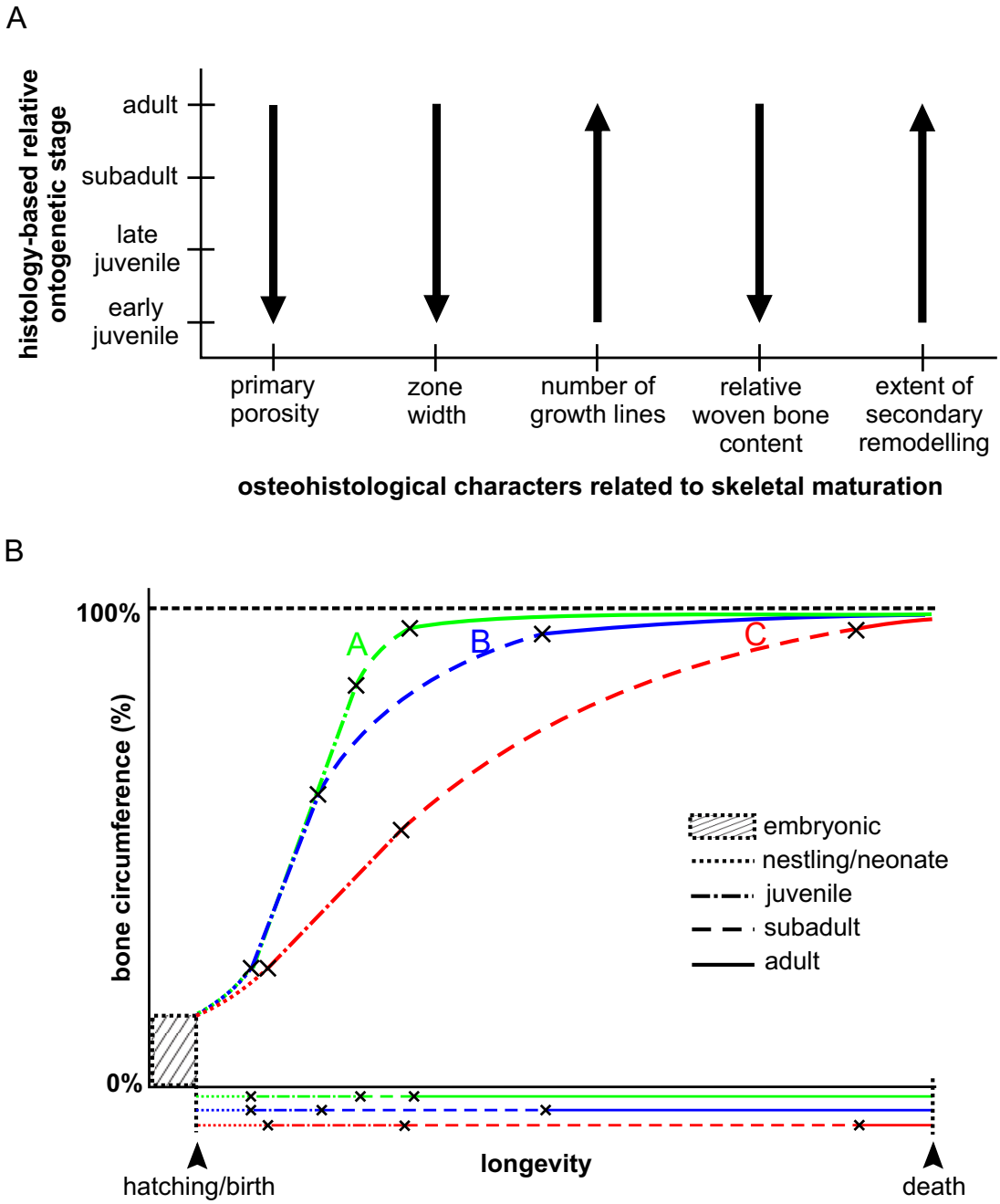

Figure 1. Theoretical assessment of size-independent ontogenetic stages based on osteohistological changes reflecting skeletal maturation (A) and the general sigmoidal relation between these ontogenetic stages and the increase in bone diameter in three different model animals(B). **A**, Expected direction of change in the selected histological characters during skeletal maturation from early juveniles to adults with the arrowheads pointing toward maximum levels. Assessing the state of these characters relative to one another is used to assign relative ontogenetic stage to the studied specimens. **B**, Demonstration of size-independent ontogenetic stages defined by skeletal maturation in three different growth strategies. Curves A, B, and C represent general 'bird'-, 'mammal'- and 'crocodile'-like growth strategies, respectively. Longevity is standardized to a relative time frame spanning from hatching or birth to death (*X*-axis), and growth is expressed as the increasing percentage of adult bone circumference (*Y*-axis) within this time range. Black crosses on the curves mark the reference points of the developmental sequence (as defined by Smith, 2001) after which the first derivatives of the respective phase of the curve sensibly change compared to those of the preceding phase due to a decrease in the diametrical bone growth rate. Hence, these growth phases represent relative ontogenetic stages, such as nestling or neonate, juvenile, subadult and adult indicated by dotted, dot-and-dash, dashed and solid lines, respectively. Corresponding ontogenetic stages on the curves A, B, and C are delineated by the same types of lines. Colour coded lines below the 'Longevity' axis are respective projections of the growth curves on this standardized time scale. These lines demonstrate the proportion of life span an animal spends in either ontogenetic stage in each growth strategy. Since this maturation process is also reflected in the microstructure of bones, histology can be used to infer relative ontogenetic stages based on the principles demonstrated for the growth dynamics of bone circumference. Note that these ontogenetic categories are not restricted to pre-set size categories, and hence achieved sizes of corresponding ontogenetic stages can vary from one individual to the other. Pre-hatching or prenatal period is not interpreted here. Differences in the course of the hypothetical general curves are deduced from Erickson & Brochu (1999); Castanet *et al*. (2000); Montes *et al*. (2005), Erickson *et al*. (2007); Cooper *et al*. (2008), and Lee & Werning (2008).

categories have considerable overlap with the histological features described for the juvenile, subadult and adult categories established by Horner *et al*. (2009), there is a fundamental difference between the two categorizations. Horner *et al*. (2009) synonymized the ontogenetic stages perinate, juvenile, subadult and adult with the four size classes they identified in their sample, and thereafter the histological features were described for each size class. Thus, the decisive factor in assigning specimens to ontogenetic stages was clearly size rather than histology. By contrast, current study uses exclusively histological characters to establish the ontogenetic stages regardless of the actual specimen sizes. Hence, these categories are defined as a developmental sequence in the sense that they are based on the histological features reflecting the general dynamics of diametric growth of the individual bones (Fig. 1B). This concept is congruent with the standardizing concept of heterochrony described by Smith (2001) where certain events in the developmental sequence are used as reference points to enable interspecific comparisons and to reveal the diversity of growth trajectories among different species. The size-based method of Horner *et al*. (2009) may circumvent the problem of allometric growth of different parts of the skeleton when assigning ontogenetic stages to individuals (e.g., a rib or a metatarsal may show already mature histological features, whereas the femur of the same specimen is still growing showing subadult characteristics in its microstructure). However, it is informative mostly if the investigated specimen is an associated skeleton with several different elements present to sample. In the case of isolated material, the best way to identify the ontogenetic stage of specimens is a histology-based categorization. The same skeletal elements should be compared; however, if there is a diverse sample of elements to investigate, it is always worth to consider and describe the histology of non-homologous bones as well. Nevertheless, when interpreting microstructural patterns in an ontogenetic context, it is important to keep the allometric growth patterns of different elements in mind.

Because of the energy allocation from growth to reproduction, the onset of sexual maturity is also expected to slow down the bone growth (e.g., Reiss, 1989; Green & Rothstein, 1991; Chinsamy-Turan, 2005; Erickson, 2005; Erickson *et al*. 2007), and thereby to match the histological definition of subadults applied in this study. However, due to the uncertainties related to reproductive strategies of extinct animals (Erickson *et al*. 2007; Lee & Werning, 2008), each of the ontogenetic categories defined here refers to the state of skeletal and not sexual maturation of the specimens. Since the development of bone follows a continuous trajectory, setting borders between developmental categories defined here (black crosses on Fig. 1) is somewhat arbitrary, and sometimes transitional categories (e.g., late juvenile-subadult) needed to be assigned to specimens with transitional histological features.

RESULTS

Revised ontogenetic stages of different rhabdodontid groups

The comparatively extensive sample size in the genus *Rhabdodon* improved our insight into bone histological details; however, at the same time it has led to some uncertainties concerning assignment of ontogenetic stages to each specimen. On one hand this is because the numerous specimens represent transitional forms that lie on a continuous ontogenetic trajectory. On the other hand, controversies arose when multiple sections were taken from the same specimen. Generally, along the long axis of one element, mid-diaphyseal sections have proven to imply the most mature developmental stage, whereas more proximal or distal sections with usually more porous outer cortex referred to less mature ontogeny. However, these differences are completely congruent with the histological features of diametrical and longitudinal growth of long bones (e.g., Haines, 1942; Enlow, 1962; Ricqlès, 1975; Francillon-Vieillot *et al*. 1990). These potential differences were taken into account while evaluating histological characters indicative of relative ontogeny. Thus, wherever available, mid-diaphyseal sections were used for ontogenetic assignment of specimens.

Although bad preservation, such as diagenetic staining and missing outermost cortex in the samples of *Zalmoxes robustus*, renders ontogenetic assignments uncertain, the ontogenetic classification of the *Zalmoxes* specimens following the concept of Stein & Prondvai (2014) and Prondvai *et al*. (2014a) is in 100% agreement with the ontogenetic assignments provided by Ősi *et al*. (2012). On the other hand, revised developmental ordering of one specimen of *Mochlodon vorosi*, one of *Mochlodon suessi*, and some specimens of *Rhabdodon* does not completely correspond with that of Ősi *et al*. (2012). The femur MTM V 2010.126.1 of *M. vorosi* is reassigned from adult to subadult stage, the scapula PIUW 3518 of *M. suessi* from late juvenile to early juvenile, and both the humerus MHN AIX PV 1999.12 and femur MHN AIX PV 2001.A3 of *Rhabdodon* sp. from early juvenile to late juvenile. Accordingly, a new graph on the relationship between the revised histology-based ontogenetic stages and estimated femur lengths (taken from Ősi *et al*. 2012) of the sampled specimens is also presented (Fig. 2). Whether different elements of corresponding ontogenetic stages could have belonged to the same animal is impossible to tell given the subjectivity in setting border between adjacent ontogenetic categories, the potential allometric development of different parts of the skeleton, and the missing or insufficient data on the exact location and position of these isolated finds. For more detailed information on the specimens and their assigned ontogenetic stages, see Table 1.

Developmental changes in bone histology of different rhabdodontids

Although discrepancies attributable to the differences in the sampled bones as well as in the locations of sampling are evident among specimens of corresponding ontogenetic categories, developmental progress in the general histology of elements of subsequent ontogenetic stages can be reconstructed.

Mochlodon.

1. Early juveniles. The earliest juvenile stages are identified among the specimens of *Mochlodon suessi*: the radius PIUW 3517 (Fig. 3A,B), femur PIUW 2349/III (Fig. 3C,D), and the scapula PIUW 3518 (Fig. 3E,F). Of these elements, the two limb bones have obviously more in common concerning their overall histology than either of them has with the scapula.

In both limb elements, the cortex is relatively thin as compared to the extensive medullary cavity. The medullary cavity of the femur shows some remnants of spongy bone (Fig. 3C,D), but the cavity is devoid of bony trabeculae in the radius (Fig. 3A). Although fast medullary expansion and perimedullar bone resorption characterize both elements, traces

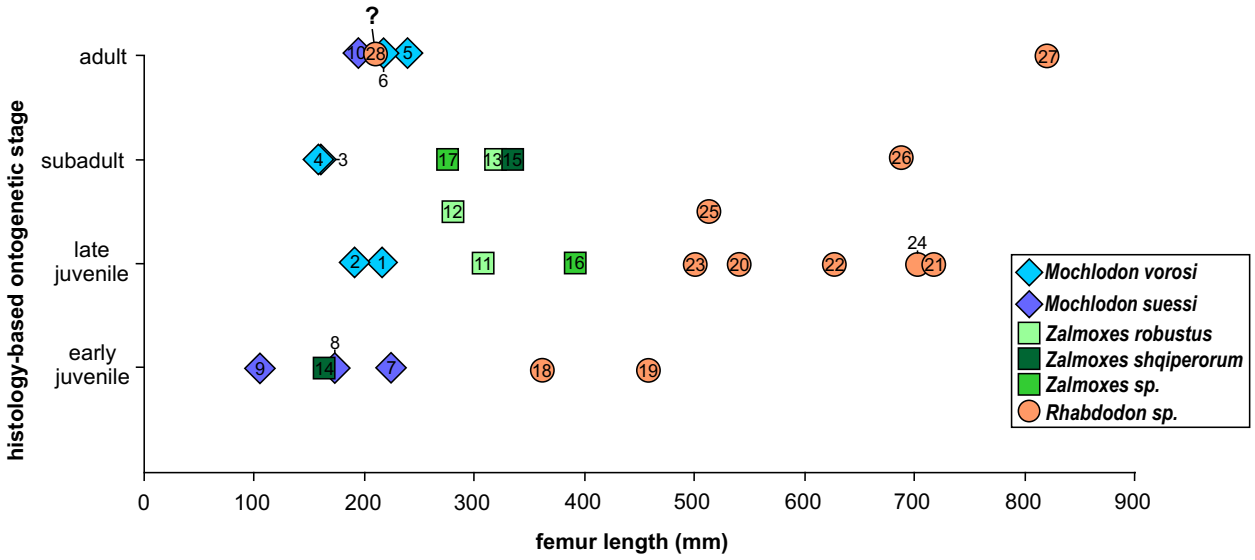

Figure 2. Relationship between histology-based ontogenetic stages and femur length in the sample of rhabdodontid specimens. Comparison of this plot with that presented by Ősi *et al*. (2012, Figure 13) shows that the early juvenile specimens of *Rhabdodon* represent a size range expected for young individuals, whereas unexpectedly large specimens were also placed into the corresponding ontogenetic category by Ősi *et al*. (2012). However, the adult femur MHN AIX PV 2008.1.11 (indicated by nr. 28 and a question mark) still represents an outlier by being in the range of adult femoral length of *Mochlodon*. Specimen – code number correspondence is given in Table 1.

of a thin layer of endosteal bone rimming the medullary cavity are discernible in the femur (Fig. 3C,D). Whereas the preserved cortex of the radius is predominantly primary with secondary remodelling mostly being restricted to the perimedullary regions, remodelling is more extensive in the femur. Here, the innermost cortical layer is remodelled sometimes by multiple generations of osteons, and in the area of the fourth trochanter secondary resorption and remodelling reach the outer surface of the bone.

The primary vascular architecture is mostly longitudinal in the radius (Fig. 3B) and more irregular in the femur with regional differences throughout the cortex in both elements. Vascular canals in the peripheral cortex are wide, and several open onto the periosteal surface. Width of the canals is locally variable, but generally they are moderately narrow in the radius and relatively wider in the femur with varying extent of lamellar compaction. Porosity of the primary cortex is higher in the femur than in the radius. There is neither a progressive change in the vascular architecture, nor a progressive decrease in vascularity towards the outermost cortex in either element.

Lines of arrested growth (LAGs) can be observed in both elements. In the radius, the three, closely spaced LAGs (triple LAG *sensu* Werning, 2012) are organized in an almost avascular annulus in the outer two-third of the cortex (Fig. 3A,B). In the femur, two faint LAGs are present in the outer cortical third (Fig. 3D), but they are not discernible all around the cortex and, apart from an apparently slight decrease in vascularity, the surrounding bone tissue shows no distinct annulus-like features.

Primary bone is a combination of woven and parallel-fibred bone, i.e. woven-parallel-complex or WPC (Prondvai *et al*. 2014a). Based on lacunar and optical features of the tissue derived from dynamic osteogenesis (DO, Marotti, 2010; and see Stein & Prondvai, 2014; Prondvai *et al*. 2014a), the orientation of the primary non-lamellar parallel-fibred bone (PFB) is mainly longitudinal in the radius and helical in the femur, but some areas show strong birefringence (Fig. 3A,D) with longitudinally cut lacunae in cross section referring to circumferential PFB. Such circumferential organization can be observed in the perimedullary region and in the annulus of the radius as well as on one side of the fourth trochanter and along the LAGs in the femur. Woven bone does not form contiguous trabeculae as in sauropod laminar bone (Stein & Prondvai, 2014), but rather nodules adjacent to the primary canals mostly in the inner, more densely vascularized cortical half. These areas contain clusters of large, randomly oriented lacunae derived from static osteogenesis (SO, Marotti, 2010). Hence, these cortical areas can be identified as fibrolamellar complex or FLC (Ricqlès, 1975) as defined by Prondvai *et al*. (2014a). The relative amount of woven bone is clearly higher in the femur than in the radius.

The fourth trochanter of the femur accounts for the most striking differences between the overall histology of the radius and femur. Apart from the diagenetic alteration causing colour pattern that clearly does not reflect the original bone microstructure, the most dominant histological feature in the primary bone of the forth trochanter is the few, unusually wide vascular canals and the extrinsic structural fibres, the latter of which make the primary matrix locally highly birefringent under crossed plane polarizers (Fig. 3D). The abundance of SO-derived lacunae in this region indicates that the incorporation of extrinsic fibres into the bone matrix happens via static osteogenesis. Numerous secondary osteons of wide lumen and larger cavities invade the entire area of the fourth trochanter. Although described as a primary structure, very similar histological features in the fourth trochanter of *Dysalotosaurus* were referred to as "Posterolateral Plug" by Hübner (2012) (Fig. 3C). This combination of microstructural features restricted to the trochanteric area clearly reflects the biomechanical importance of the trochanter as a major muscle attachment site on the femur and says less about the relative ontogenetic status of the specimen itself.

In sum, the general microstructure of the radius exhibits

more mature features than that of the femur which either indicates the earlier ontogenetic stage of the femur or reflects the allometric growth of these different skeletal elements.

In the scapula PIUW 3518 of *M. suessi*, the identification of the original tissue types is more difficult due to extensive diagenetic alterations. Nevertheless, the most characteristic microstructural features can still be discerned. The spongy bone of the medullary cavity gradually merges into the compacta with progressively smaller erosion cavities (Fig. 3E). Scattered secondary osteons reach up to the half of the cortex, whereas the outer half is mainly primary. The moderately wide primary vascular canals are mostly longitudinal, but there are regional

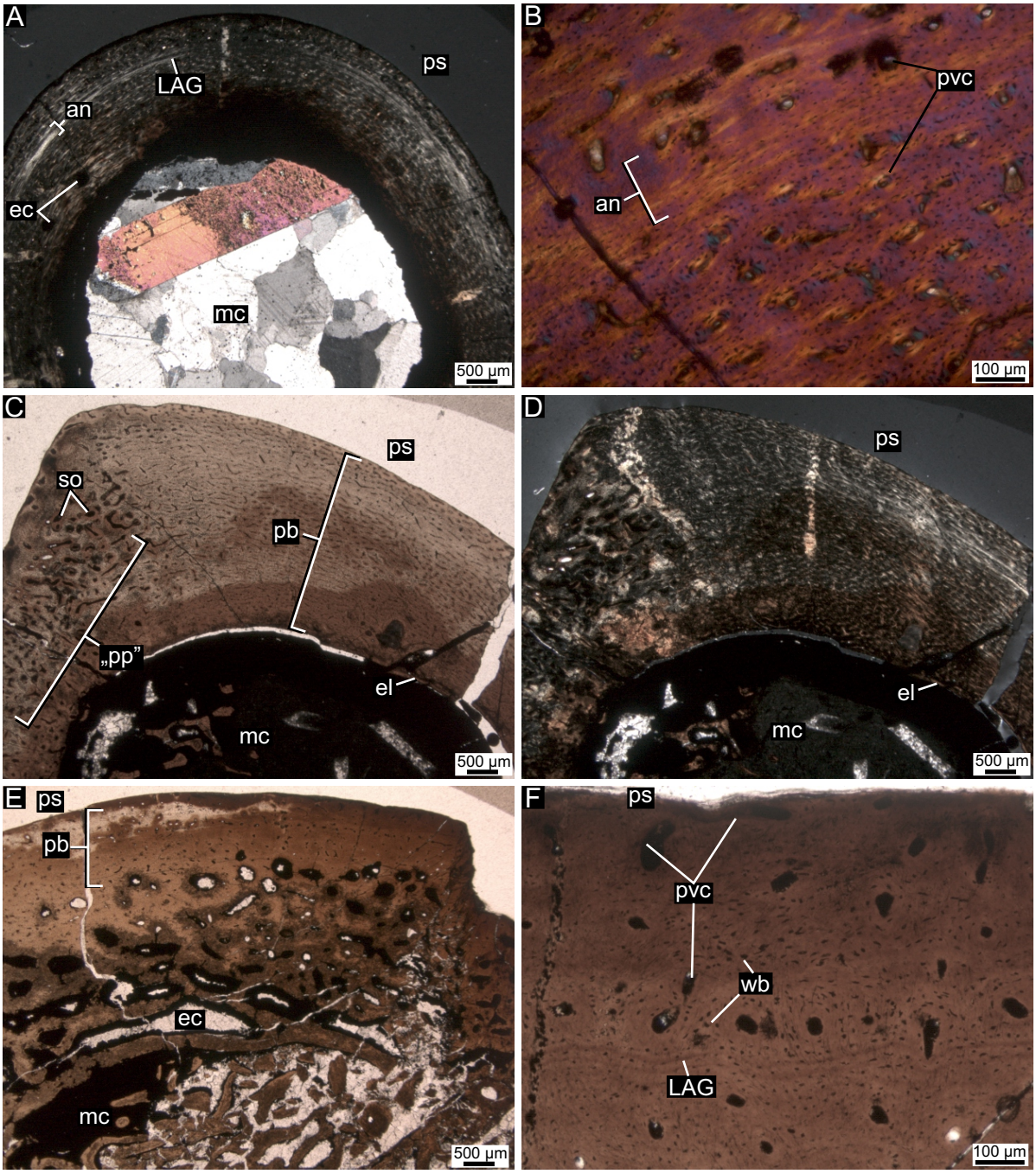

Figure 3. Transverse thin sections of the early juvenile radius PIUW 3517 (A,B), femur PIUW 2349.III (C,D), and scapula PIUW 3518 (E,F) of *Mochlodon suessi* under cross polarized light (A,D) aided by λ wave plate (B), and under plane polarized light (C,E,F). **A**, Overview on one half of the complete cross section of the radius revealing the large medullary cavity relatively to cortex thickness, and a thin annulus with a double LAG and circularly oriented fibres appearing bright. Larger erosion cavities are present in the inner cortical half. **B**, Close-up of the less densely vascularized annulus contrasting with the underlying layer with dense longitudinal primary vascular canals. **C** and **D**, Overview on nearly half of the complete cross section of the femur showing the very distinct microstructure in the area of the fourth trochanter that was referred to as "Posterolateral Plug" by Hübner (2012). In this area, numerous secondary osteons invade the outermost cortex, whereas they are completely missing from the bulk of the primary cortex elsewhere. **E**, The majority of the cortex of the scapula is primary; however, large erosion cavities reach up to the cortical half. These cavities progressively increase in size towards the medullary cavity. **F**, Close-up of the well-vascularized periosteal surface with patches of woven bone adjacent to primary vascular canals and a double LAG running close to the surface.

differences in the vascular architecture and density as well. No tendency of decrease in vascularity towards the periosteal cortex can be detected, and numerous vascular canals still open on the periosteal surface (Fig. 3F). One growth mark can be observed running half way in the thickness of the primary cortex and consists of two closely packed LAGs (double LAG *sensu* Werning, 2012) (Fig. 3F). Spindle shaped lacunae along the LAGs in the transverse section refers to circumferentially oriented PFB, whereas most other regions show characteristics of longitudinal PFB (see Stein & Prondvai, 2014; Prondvai *et al*. 2014a). Extrinsic fibres associated with SO-derived lacunae determine the primary structure of certain cortical areas. Patches of woven bone are present and frequent across the entire primary cortex (Fig. 3F) which is thus defined as WPC.

In conclusion, in all early juvenile elements, changes in overall histology refer to cyclicity rather than to a progressive developmental sequence that usually characterizes more mature ontogenetic stages.

2. Late juveniles. The more mature ontogenetic stage defined here as late juvenile is represented by two specimens of *Mochlodon vorosi*, the femur MTM 2012.25.1 (Fig. 4A,B) and the tibia MTM 2012.26.1 (Fig. 4C,D).

Although, the exact extent of the medullary cavity cannot be determined in either of these elements, the relative thickness of the cortex is clearly greater than that of the early juvenile radius PIUW 3517 (Fig. 3A,B) and femur PIUW 2349/III (Fig. 3C,D). Remnants of a thin endosteal layer rimming the medullary cavity can be observed in both the femur MTM 2012.25.1 and the tibia MTM 2012.26.1. Secondary remodelling is locally very extensive with secondary osteons invading the outer third of the cortex in the tibia (Fig. 4D), and the outermost cortex at the fourth trochanter in the femur (Fig. 4A). In fact, secondary remodelling at the fourth trochanter is extreme and represented on one hand by obliquely cut or radial secondary osteons, and on the other hand by sometimes two generations of more ordinary longitudinal osteons. The lumen of some of these osteons is surprisingly wide accounting for the high porosity of this area (Fig. 4A). Here, only very restricted patches of primary bone can be distinguished referring to the more mature ontogenetic state of this femur compared to PIUW 2349/III.

In both limb bones, primary vascular density is comparatively high, but vascular canals are well compacted having narrow lumen, consequently the overall porosity is apparently lower than in the early juveniles. Lamellar development around primary vascular canals is present; however, not pronounced. Vascular canals run mainly longitudinally with a number of short circumferential anastomoses. There is no change in

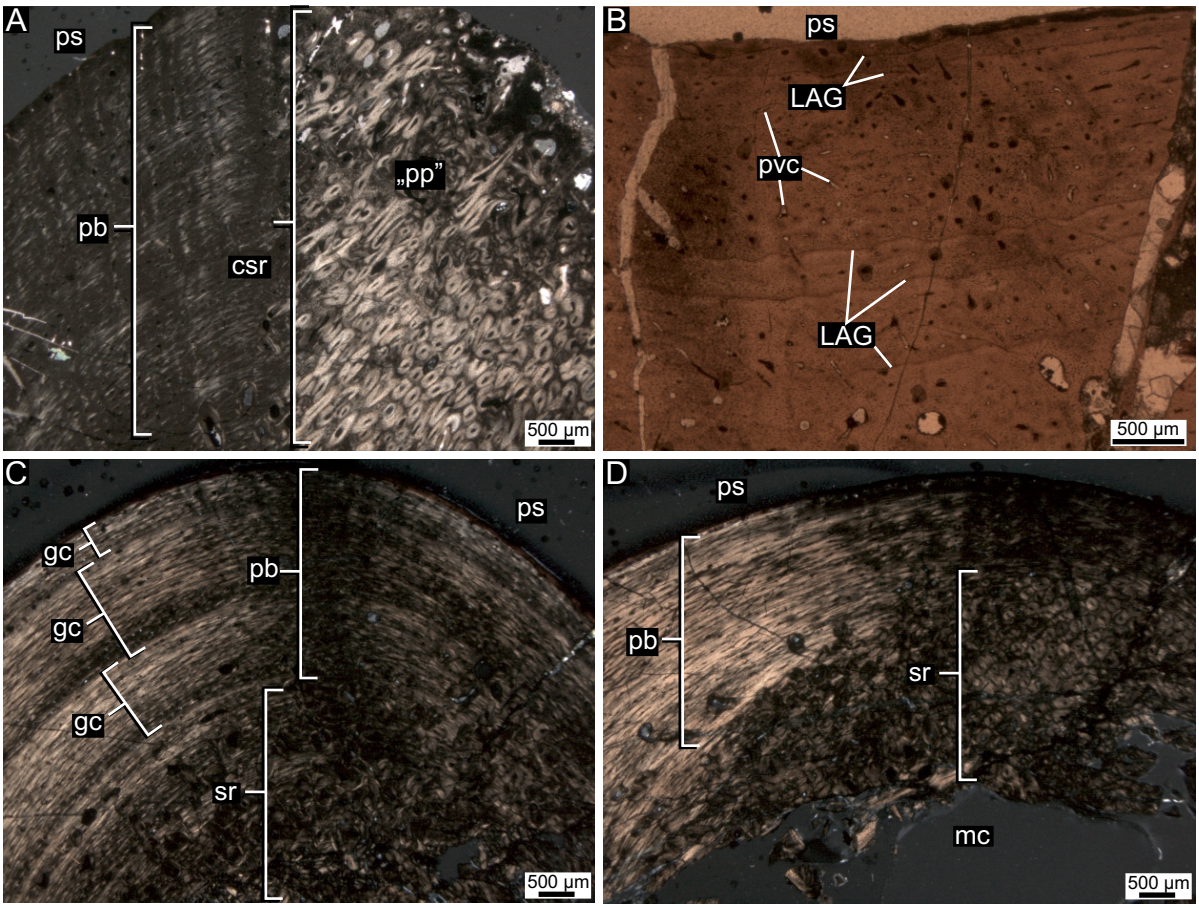

Figure 4. Late juvenile femur MTM 2012.25.1 (A,B) and tibia MTM 2012.26.1 (C,D) of *Mochlodon vorosi* in transverse section under crossed plane (A,C,D) and single plane (B) polarizers. **A**, At the level of the fourth trochanter, this femur exhibits sudden interruption of primary bone with complete secondary remodelling in the "Posterolateral Plug" (Hübner, 2012). **B**, Primary cortex at the periosteal surface reveals a number of irregularly spaced LAGs and mostly longitudinal primary vascular canals. Neither vascular features, nor LAGs show any tendentious changes towards the periosteal surface. **C**, The thickest part of the cortex showing considerable remodelling by secondary osteons mostly in the inner third of the compacta. The outer two-third of the cortex is primary, almost exclusively parallel-fibred bone and exhibits growth marks referring to growth cycles with large amount of bone deposited between the subsequent lines. **D**, Locally, in the thinner cortical half secondary remodelling reaches up to the external third of the cortex.

vascular architecture or density peripherally in either of the limb bones, and several vascular canals are connected with the periosteal surface indicating active diametrical bone growth at the time of death (Fig. 4B).

Five to six intracortical LAGs are present in both elements with even or slightly variable spacing (Fig. 4B).

The preserved primary cortex is WPC in the femur and almost exclusively PFB in the tibia. The non-lamellar PFB in the femur apparently changes orientation across the section. In cross section, the medial half of the primary matrix shows intermediate birefringence that becomes stronger along the LAGs implying an essentially helical PFB that adopts a more circumferential orientation adjacent to the LAGs (Fig. 4A). However, the lateral half, that is separated from the medial half by scattered secondary osteons in the poorly preserved anterior area, shows optical and lacunar features that are characteristic of essentially longitudinal PFB. The majority of PFB in the transverse section of the tibia has medium to high birefringence, i.e., helical to circumferential orientation with a very thin layer of longitudinal PFB following some LAGs that stays dark under cross polarized light (Fig. 4C). Woven bone content is almost zero in the tibia, and generally low in the femur with sparse nodules of SO-derived lacunae which are the most frequent in the remnant areas of primary bone of the fourth trochanter region.

Just like in early juveniles, both specimens identified here as late juveniles show cyclical changes in their histology with no clear indication of progressive decrease in diametrical bone growth rate.

3. Subadults. Two *Mochlodon* specimens show histological features characterizing them as subadults: the femur MTM V 2010.126.1 (Fig. 5A) and the tibia MTM V.01.101 (Fig. 5B) of *M. vorosi*. The bone microstructure of these elements is clearly more mature than that of any late juveniles with indication of drastic slowing down of growth but with some diametrical growth still possible. Although they represent different skeletal elements, and the microstructural preservation state of the tibia is very poor, the histology of these bones shows almost identical features.

The medullary cavity is crushed in the femur and not preserved in the tibia, therefore its relative extent and general structure cannot be described. The innermost cortex of both elements is severely damaged and therefore not to be determined. The majority of the preserved cortex in both elements is of primary origin. Locally, however, the femur is invaded by scattered secondary osteons of wide lumen up to the outermost cortex (Fig. 5A) and the tibia is heavily remodelled by multiple generations of osteons throughout the cortical width except the outermost layer adjacent to the periosteal surface (Fig. 5B). In general, the inner half of the preserved cortex in the femur contains some large secondary erosion rooms, and a few secondary osteons that also occur in the more peripheral cortical regions.

Vascularity is very sparse throughout the primary cortex in both elements with mostly longitudinally running, almost completely filled primary vascular canals (Fig. 5). However, no considerable amount of lamellar component can be observed in the primary osteons. In the tibia, more transverse anastomoses are present in the inner than in the outer half of the preserved cortex (Fig. 5B), whereas there is no such tendency in the vascular architecture of the femur. Vascular density as well as porosity clearly decreases peripherally in the tibia; however, this large scale trend is not apparent in the femur.

Up to five and ten intracortical growth marks are present in the femur and tibia, respectively. These growth marks are fainter and more distantly spaced in the inner half and more pronounced and densely packed in the outer half of the cortex. The width of the zones between LAGs decreases suddenly in the femur (Fig. 5A) and progressively in the tibia towards the periosteal surface (Fig. 5B); however, some growth marks in the deeper cortex are not as distinct as to be identified as LAGs. This along with the substantially decreasing vascularity in the tibia refers to the onset of the formation of an external fundamental system or EFS that eventually would have resulted in the complete cessation of growth in both elements. However, in the tibia, there is an avascular annulus with multiple LAGs visible in the outer third of the cortex that is still followed by an extensive deposition of primary bone, and the outermost cortex of both elements still contains a considerable number of vascular canals. These suggest that, even if at a much slower rate, further diametrical bone growth was possible when the animal(s) died verifying the subadult nature of these elements.

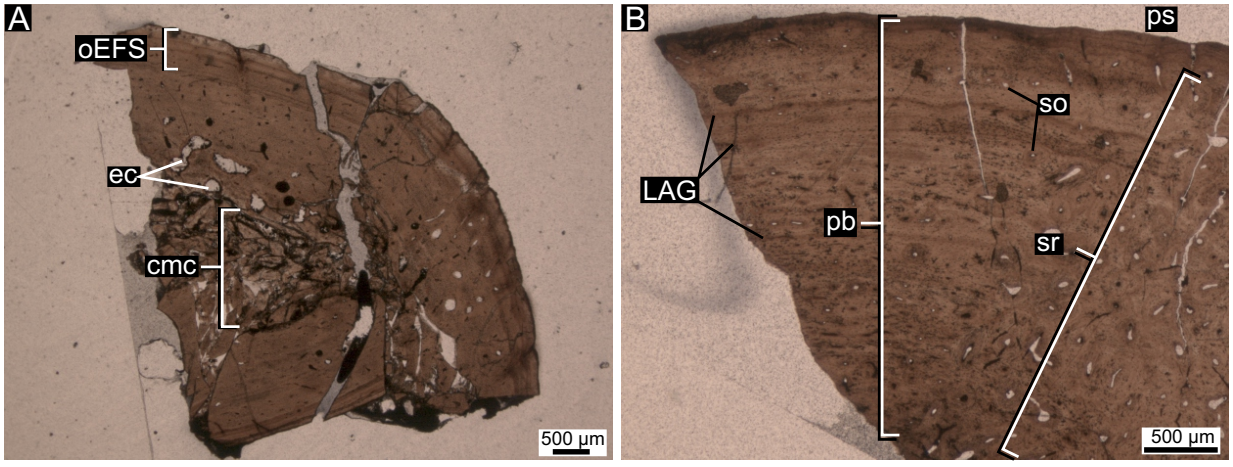

Figure 5. Transverse thin sections of the subadult femur MTM V 2010.126.1 (A) and tibia MTM V 01.101 (B) of *Mochlodon vorosi* under plane polarized light. **A**, Most of the femoral cortex is primary with small, predominantly longitudinal canals and some perimedullary erosion cavities. The onset of an external fundamental system is evident. The medullary cavity is crushed. **B**, Cortex showing closely spaced LAGs and sparse longitudinal vascular canals with small lumen. Secondary remodelling reaches the outer surface.

Primary bone is WPC in the femur but its fine microstructure is hard to discern in the tibia. In the cross section of the femur, primary bone has mostly moderate birefringence with obliquely cut DO-derived osteocyte lacunae suggesting helically oriented PFB with no distinct change in this orientation along the LAGs. Because of the poor preservation, neither the optical nor the lacunar features are reliable enough to describe the structural organization of the PFB in the tibia. Locally in the femur, bundles of Sharpey's fibres enter the cortex obliquely, protruding in the deepest preserved cortical regions too. Extrinsic fibres seem to be the most abundant in the area of stronger secondary remodelling. In these regions, the osteocyte lacunae appear larger and randomly shaped and oriented suggesting that the extrinsic fibres are embedded into a framework of woven bone,

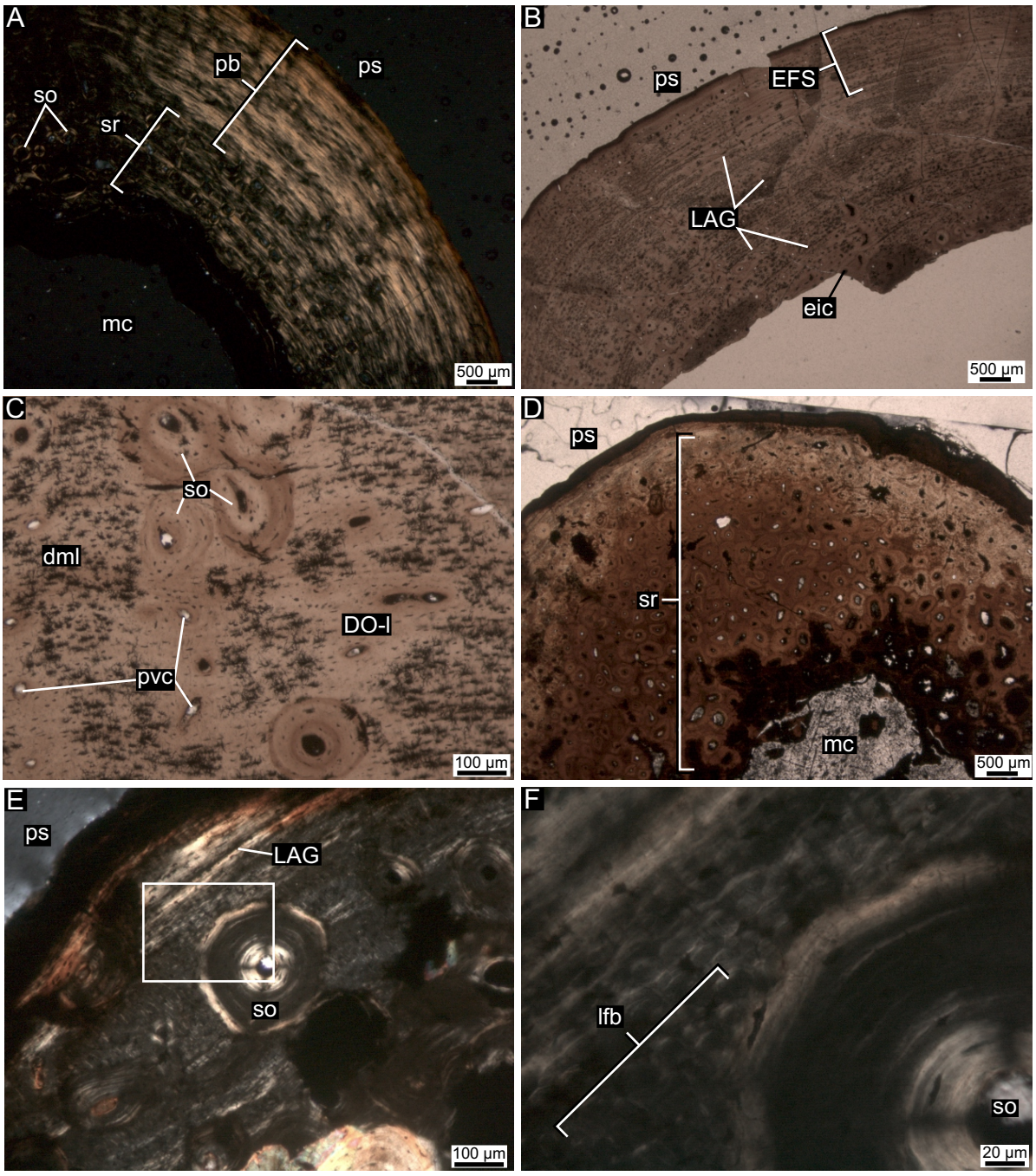

Figure 6. Transverse section of adult humerus MTM 2012.23.1 (A) and femur MTM V 01.225 (B,C) of *Mochlodon vorosi*, and tibia PIUW 2349/35 (D-F) of *M. suessi* under crossed plane (A,E,F) and single plane (B-D) polarizers. **A**, Primary cortex in the humerus consists mostly of circularly oriented parallel-fibred bone that shows strong birefringence. Secondary osteons reach up to the cortical half. **B**, The majority of the femoral cortex is primary with scattered secondary osteons and a large number of closely spaced LAGs, although the inner cortex is eroded. The outermost cortex is almost avascular and is interpreted here as showing an EFS. **C**, Close-up of the inner cortical part with diagenetically modified lacunae in the primary bone and with scattered secondary osteons. **D**, Apart from a very thin outermost primary layer, the entire cortex of the tibia is secondarily remodelled by multiple generations of secondary osteons. **E**, The preserved outermost primary bone layer is restricted to a small area around the circumference of the bone and shows a distinct LAG that is part of an EFS obscured by diagenetic staining. White square indicates the relative position of the magnified area shown in F. **F**, Bundles of longitudinally running structural fibres right next to a large secondary osteon with circular and longitudinal fibre orientation in the inner and outer half, respectively.

just like in the fourth trochanter of the femora PIUW 2349/III and MTM 2012.25.1. The most extensive patches of woven bone are present in these areas, whereas they are exceptionally sparse and consist only of a few SO-derived lacunae in the innermost cortical areas.

4. Adults. In total, three *Mochlodon* specimens are identified as adults, two of *M. vorosi*, the humerus MTM 2012.23.1 (Fig. 6A) and the femur MTM V.01.225 (Fig. 6B,C), and one of *M. suessi*, the tibia PIUW 2349/35 (Fig. 6D-F). Whereas the femur and humerus of *M. vorosi* exhibit almost identical histology, the tibia of *M. suessi* has a fundamentally different bone microstructure.

The medullary cavity of the humerus is void of trabeculae. However, a thin layer of endosteal bone can be observed being detached from the perimedullary cortex in the latter of which very few erosion cavities and much more secondary osteons are visible. Secondary remodelling in the innermost cortex is locally different with areas of sparse, scattered secondary osteons as well as of dense remodelling sometimes with multiple generations of osteons (Fig. 6A). The perimedullary region of the femur is missing from the section and the preserved cortex is mainly primary bone (Fig. 6B). However, secondary osteons locally invade the peripheral cortex, and are more frequent in the deeper cortical regions of the femur too indicating that the inner cortical half was most likely considerably remodelled.

In both elements, the structure of the primary bone implies a slow, varanid-like accretional diametrical growth (Buffrenil *et al*. 2008) throughout the period in which the preserved primary cortex was being deposited. The primary vascular architecture is almost exclusively longitudinal with very sparse and narrow vascular canals with no considerable amount of lamellar infilling. This extremely low vascular density and cortical porosity gives an almost avascular appearance for the entire primary cortex (Fig. 6A,B), although the progressive decrease in vascular density towards the periosteal surface is locally still detectable in the humerus.

Intracortical LAGs (i.e. not part of an EFS, as used by Erickson et al. [2007, 2009]) are very abundant throughout the cortex in both elements (up to 9 and 14 in the humerus and femur, respectively) and become even more densely packed towards the periphery eventually forming an avascular EFS (Fig. 6B). In the humerus the scarce longitudinal canals, where present, are aligned in more or less circumferential rows between two adjacent LAGs.

The primary bone in the humerus shows cyclically changing optical behaviour with alternating low and high birefringence in cross section. High birefringence mostly matches the

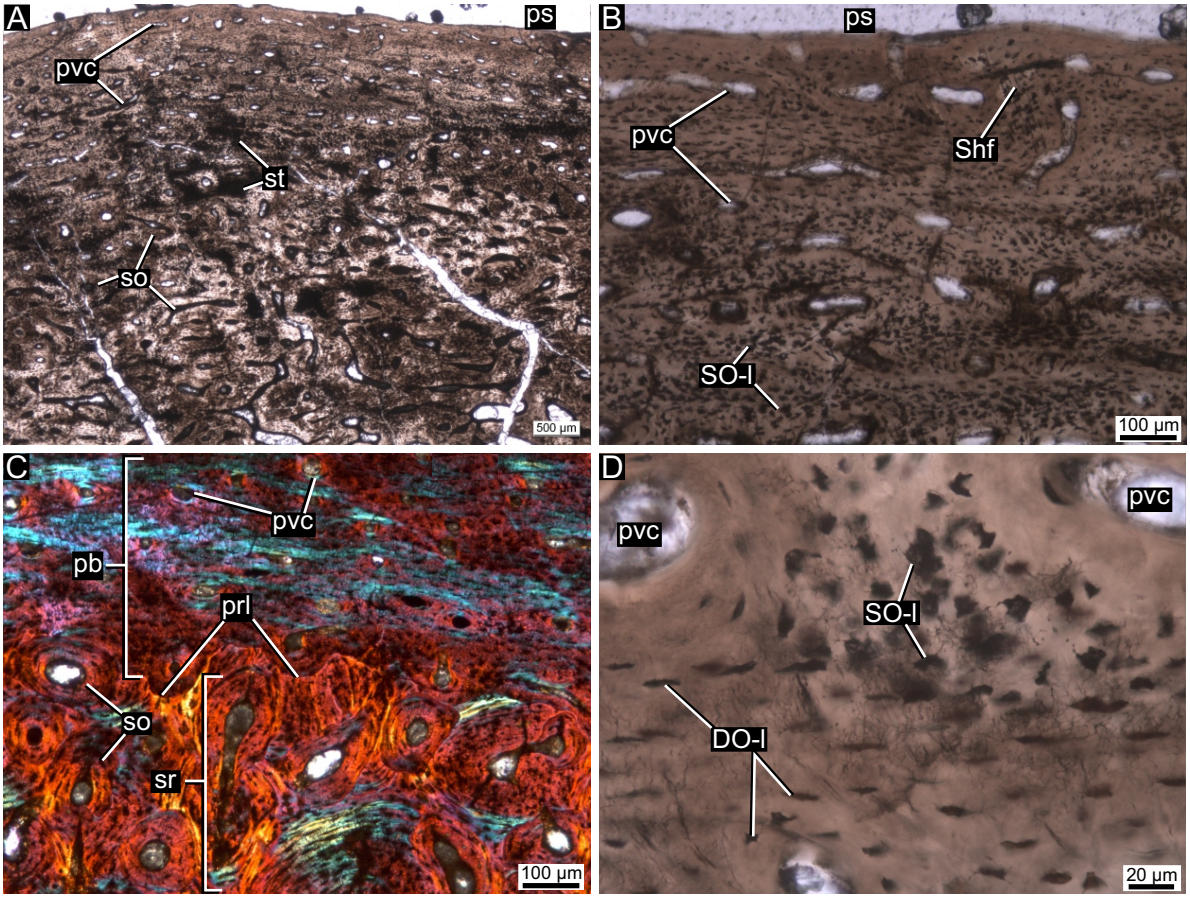

Figure 7. Transverse sections of the early juvenile femur R.1088 of *Zalmoxes shqiperorum* under plane polarized light (A,B,D) and cross polarized light with λ wave plate (C). **A**, Even though more than half of the cortex is secondary remodelled, this remodelled region is densely vascularized with high number of longitudinally and transversely oriented secondary osteons of wide lumen. Large dark areas are the result of diagenetic staining. **B**, The peripheral cortex has wide open, longitudinal and short circular vascular canals. Woven bone content is very high with numerous SO-derived lacunae defining the cortex as fibrolamellar complex or FLC. **C**, A distinct periosteal resorption line cross-cutting the older, secondarily remodelled cortex can be observed, hence the outermost periosteal cortex can be considered as being secondary (Prondvai et al. 2014a). **D**, Details of SO- and DO-derived lacunae between adjacent primary vascular canals.

spatial arrangement of LAGs, whereas the zones in between remain almost completely dark under crossed plane polarizers. Morphology of DO-derived lacunae confirms an essentially alternating pattern of longitudinal PFB in the zones and circumferential PFB along the LAGs. In contrast to the humerus, most of the primary bone is diagenetically strongly altered in the femur obscuring the original optical behaviour and lacunar characteristics of PFB (Fig. 6C). Nevertheless, the observable DO-derived lacunar features show mostly an obliquely cut morphology, whereas adjacent to the LAGs they are sectioned along their long axis. These indicate a helical PFB in the majority of the primary bone, and a more circumferential PFB orientation along the LAGs. In the humerus, the innermost primary cortex contains a large number of SO-derived osteocyte lacunae, whereas DO-derived lacunae prevail in the outer cortical half. Thus, woven bone content drastically decreases towards the periosteal bone surface recording an ontogenetic transition from WPC to PFB.

In contrast to the general pattern found in the humerus and femur, almost complete remodelling by multiple generations of osteons characterizes the cortical histology of the tibia (Fig. 6D). The only continuous area of primary bone is represented by a very thin layer in the outermost cortex and is limited to one side of the section where it is clearly avascular and shows at least three, closely spaced LAGs (Fig. 6E). Large fibre bundles run longitudinally with transversely cut osteocyte lacunae along them. These may well represent tendinous structures embedded in the primary matrix (Fig. 6F). However, in those parts of the outermost cortex where preservation is good enough to discern such details, the majority of PFB is apparently oriented circumferentially. These features all indicate the presence of EFS that has partially been destroyed by secondary remodelling.

Zalmoxes.

1. Early juvenile. Among specimens of the genus *Zalmoxes*, the femur R.1088 (Fig. 7) of *Z. shqiperorum* is found to represent the earliest developmental stage. The section of this femur shows that the cortex – medullary cavity transition is continuous with progressively larger erosion rooms turning into a trabecular system of endosteal bone and secondary osteons in the medullary region. The extensive remodelling of the inner half of the cortex refers to a relatively early onset of secondary remodelling during ontogeny, as opposed to the conclusions of Benton *et al*. (2010). Although the outer cortical half would be usually described as primary bone, there is a clear, irregularly running periosteal resorption line that cross-cuts the secondarily remodelled inner half of the cortex (Fig. 7C). Hence, the younger outer periosteal cortex which was deposited on the older remodelled inner cortex must, per definition, be considered secondary (Prondvai *et al*. 2014a).

The primary vascular architecture in this secondary periosteal cortex is mainly longitudinal with some transverse anastomoses and wide open vascular canals resulting in a relatively high cortical porosity (Fig. 7A,B). In the deepest primary cortex, a higher number of circularly and irregularly oriented transverse vascular canals is evident. Lamellar compaction of the primary cavities is generally weak. No distinct LAG can be identified throughout the cortex; however, regionally a faint growth mark appears close to the outer surface.

The primary and secondary periosteal bone is FLC; i.e., woven bone is very extensive and frequent throughout the cortex (Prondvai *et al*. 2014a) indicating fast volume expansion of the growing bone (Fig. 7B,D). The non-lamellar PFB component shows medium birefringence with mostly obliquely cut DO-lacunae in cross section suggesting its helical orientation.

2. Late juveniles. Two *Zalmoxes* specimen can be qualitatively categorized as late juveniles, the humerus R.1392 (Fig. 8A-E) of *Z. robustus* and the humerus OB 3077 (Fig. 8F,G) of an indetermined *Zalmoxes* species. These specimens still show juvenile histological characteristics but are clearly more mature than the early juvenile femur R.1088. All microstructural features of both humeri imply that these bones did not grow as fast at the time of death as the earlier juvenile femur R.1088; however, they were still in a fast and steady growth phase without exhibiting any sign of progressive slowing down of growth.

The cortical microstructural preservation of R.1392 is better than that of OB 3077; however, the outermost surface seems to have been eroded to some extent in R.1392 (Fig. 8A). In R.1392, the medullary cavity and the cortex are distinctly separated by an endosteal layer of secondary bone (Fig. 8D) along which there are some large erosion cavities in the innermost cortex. Although the perimedullary region is poorly preserved in OB 3077, the discernible microstructure of the preserved inner cortical half implies a similar original histology as seen in R.1392. In both humeri, the extent of secondary remodelling is regionally different but always strong in the inner cortical half (Fig. 8B,C) and progressively decreases towards the periosteal surface. Scattered secondary osteons usually do not reach up to the outermost cortex. Compacted coarse cancellous bone occurs along the endosteal layer in R.1392 (Fig. 8C).

Both humeri show mostly longitudinally orientated primary vascular canals with some transverse anastomoses. However, whereas in R.1392 circular orientation is the prevalent pattern among transverse canals (Fig. 8A,E), irregular anastomoses characterize OB 3077 (Fig. 8G). In both elements, the primary vascular canals have a moderately wide lumen (Fig. 8A,G), and the lamellar component is feeble in the primary osteons. Neither vascular density nor orientation changes peripherally in the cortex (Fig. 8A,F,G).

Intracortical LAGs are distinct in the primary cortex of both specimens (Fig. 8A,F). Four to six, evenly spaced LAGs can be observed in OB 3077, while the spacing of the six, clearly discernible LAGs in R.1392 does not show any clear tendency (i.e., closely packed and distantly spaced LAGs are alternating quite randomly, see Fig. 8A).

Primary bone is WPC in both specimens. Although woven bone content is considerable (Fig. 8E), it is sensibly lower in both humeri than in the early juvenile femur R.1088, and cannot be considered FLC (*sensu* Prondvai *et al*. 2014a). In R.1392, the optical behaviour of PFB in cross section is locally different from low to high birefringence referring to changing structural organization from more longitudinal to more circumferential, respectively (Fig. 8B). The DO-derived osteocyte lacunae cut in various planes across the thin section also supports this interpretation (Fig. 8E). The birefringence of the PFB is low to intermediate in OB 3077 which suggests a longitudinal to helical PFB orientation (Fig. 8G). However, preservation of lacunar features is very poor in OB 3077, therefore lacunar orientation can neither confirm nor confute the suggested PFB orientation.

3. Late juvenile – subadult. The femur R.1382 (Fig. 9) of *Zalmoxes robustus* is a good example to show that there is no clear boundary between subsequent qualitative histology-based ontogenetic categories, as this specimen shows intermediate features in the combination of histological characteris-

tics defined for late juveniles and subadults.

Apart from the extensive network of microcracks and the missing outermost cortex (Fig. 9), the histology of this femur is comparatively well preserved. Although no medullary structures are visible in the section, the cortex seems to be distinct from the medullary cavity (Fig. 9A,B,D). Extensive secondary remodelling by multiple generations of osteons characterizes the inner cortical half, whereas the outer half is only invaded by scattered secondary osteons (Fig. 9B,D). The preserved outermost layer of the primary cortex is almost void of secondary remodelling.

The overall microstructure of the primary bone refers to slow growth at least in the period that is represented in the preserved primary growth record. The initial vascular architecture can only be observed in the outermost cortex where it is mostly longitudinal with some short circumferential anastomoses (Fig. 9C). Primary canals are of moderately narrow lumen, and vascular density is low compared to the late juveniles of *Zalmoxes*.

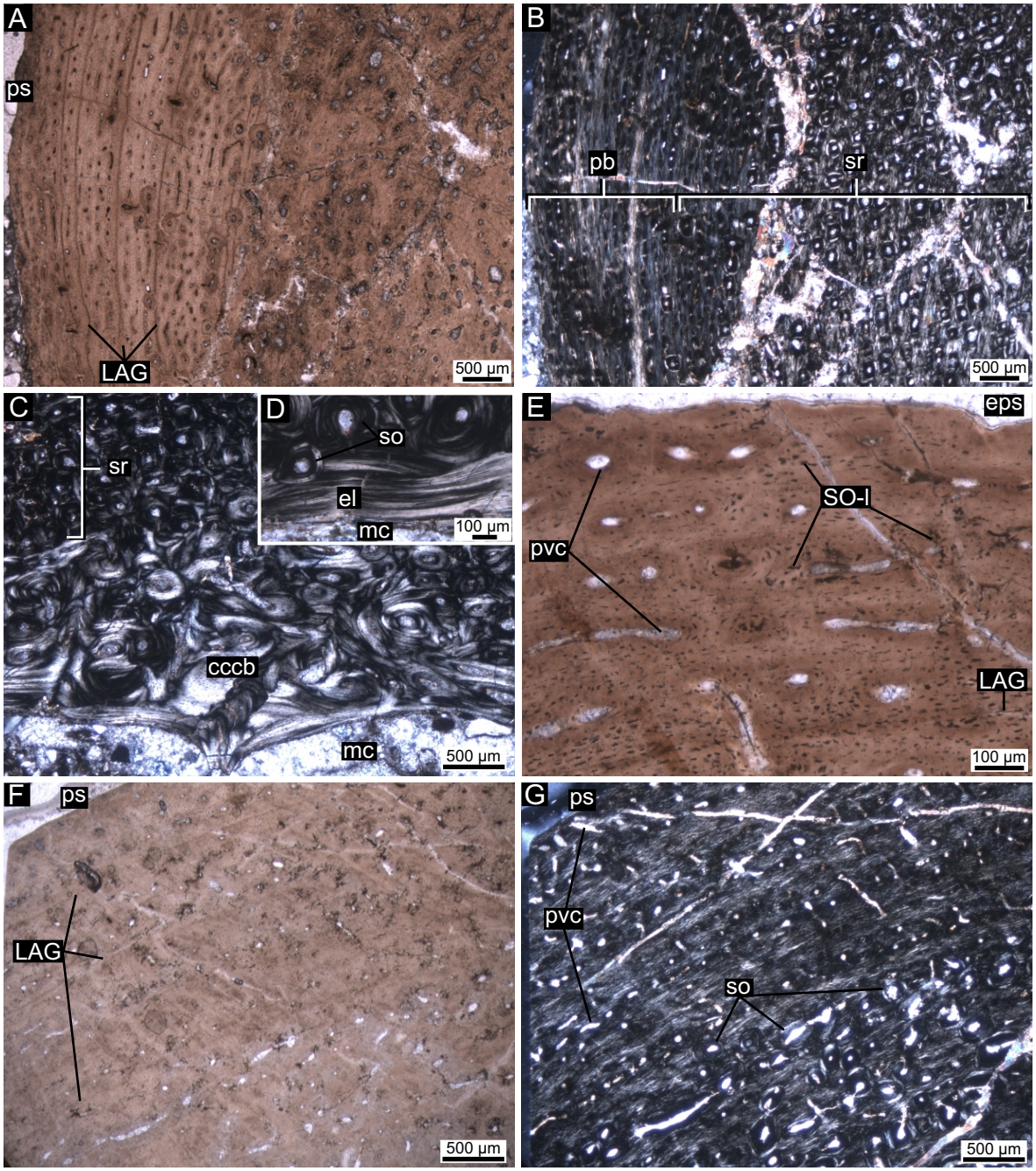

Figure 8. Late juvenile humeri R.1392 of *Zalmoxes robustus* (A-E) and OB 3077 of *Zalmoxes* sp. (F,G) under plane (A,E,F) and crossed plane polarizers (B-D,G). **A** and **B**, Two-third of the humeral cortex is secondarily remodelled, whereas primary bone in the outer third shows abundant and wide primary canals, and numerous distantly but irregularly spaced LAGs. **C**, Secondary remodelling is considerable in the inner cortical half with some compacted coarse cancellous bone present in some perimedullary areas. **D**, Locally thick endosteal layer lines the medullary cavity. **E**, Close-up of the periosteal bone layer revealing longitudinal and short circumferential primary vascular canals and scattered patches of woven bone indicated by SO-derived lacunae. **F** and **G**, The outer cortex shows sparse vascularity with mostly longitudinal primary canals of moderately narrow lumen. Scattered secondary osteons reach up to the outer third of the cortex. Faint, distantly spaced LAGs run in the primary bone.

The primary osteons have low amount of lamellar component. Changes in primary vascular features towards the periphery in the preserved thin primary cortex cannot be observed (Fig. 9C).

Ten to twelve LAGs run throughout the cortex the innermost ones of which are partially destroyed by secondary remodelling. Their spacing is variable without showing the tendency of considerably decreasing zone widths towards the periosteal surface (Fig. 9C), the latter of which would characterize subadult individuals.

The majority of the primary bone in the transverse section has moderate to high birefringence with the highest brightness usually detected along the LAGs suggesting a helical to circumferential orientation of PFB (Fig. 9D). This is in agreement with the mostly obliquely and longitudinally cut DO-derived lacunae. Woven bone in the WPC is very scarce containing only a few SO-derived lacunae that form small patches dispersed between some of the primary vascular canals.

4. Subadults. Three subadults are recognized among the *Zalmoxes* specimens, the femora R.1002 (Fig. 10A,B) and R.1608 (Fig. 10C,D) of *Z. robustus* and *Z. shqiperorum*, respectively, and the humerus R.6 (Fig. 11) which has been assigned to *Z. robustus* with a question mark but is referred to here as *Zalmoxes* sp.. The subadult nature of R.1002 is rather uncertain, because the outermost cortex is broken off, and the section is too thick and strongly affected by diagenetic staining for the observation of fine histological details (Fig. 10A). Although identified as representing two different species of *Zalmoxes*, the two subadult femora of *Z. robustus* and *Z. shqiperorum* show almost identical histology that is considerably different from the microstructure of the subadult humerus of *Zalmoxes* sp.

In both femora, the cortex – medullary cavity transition is continuous with progressively larger resorption cavities inwards that eventually become part of the endosteal trabecular system. Surprisingly weak remodelling by scattered secondary osteons characterizes the inner third of the cortex (Fig. 10C). Thus, primary bone is extensive even in the innermost cortical areas, and it definitely dominates the outer two-third of the cortex in both specimens. Nevertheless, scattered secondary osteons reach up to the outer cortical region leaving only a thin layer of primary cortex void of remodelling (Fig. 10C,D).

The structure of the primary cortex refers to an irregularly interrupted, slow diametrical bone growth in these two femora. Primary vascular canals are very sparse, well compacted and mostly longitudinal in the majority of the cortex. However, they are comparatively wide in the outermost thin layer where some even open onto the periosteal surface (Fig. 10B,D). Lamellar development in primary canals is generally weak.

At least 13 and 17, closely spaced LAGs are present throughout the cortex of R.1608 and R.1002, respectively. Although growth marks seem to become denser in the outermost cortical layer, due to the general abundance and density of LAGs throughout the cortex and the overall sparse vascularity, the presence of an EFS cannot be confirmed (Fig. 10). In addition, based on

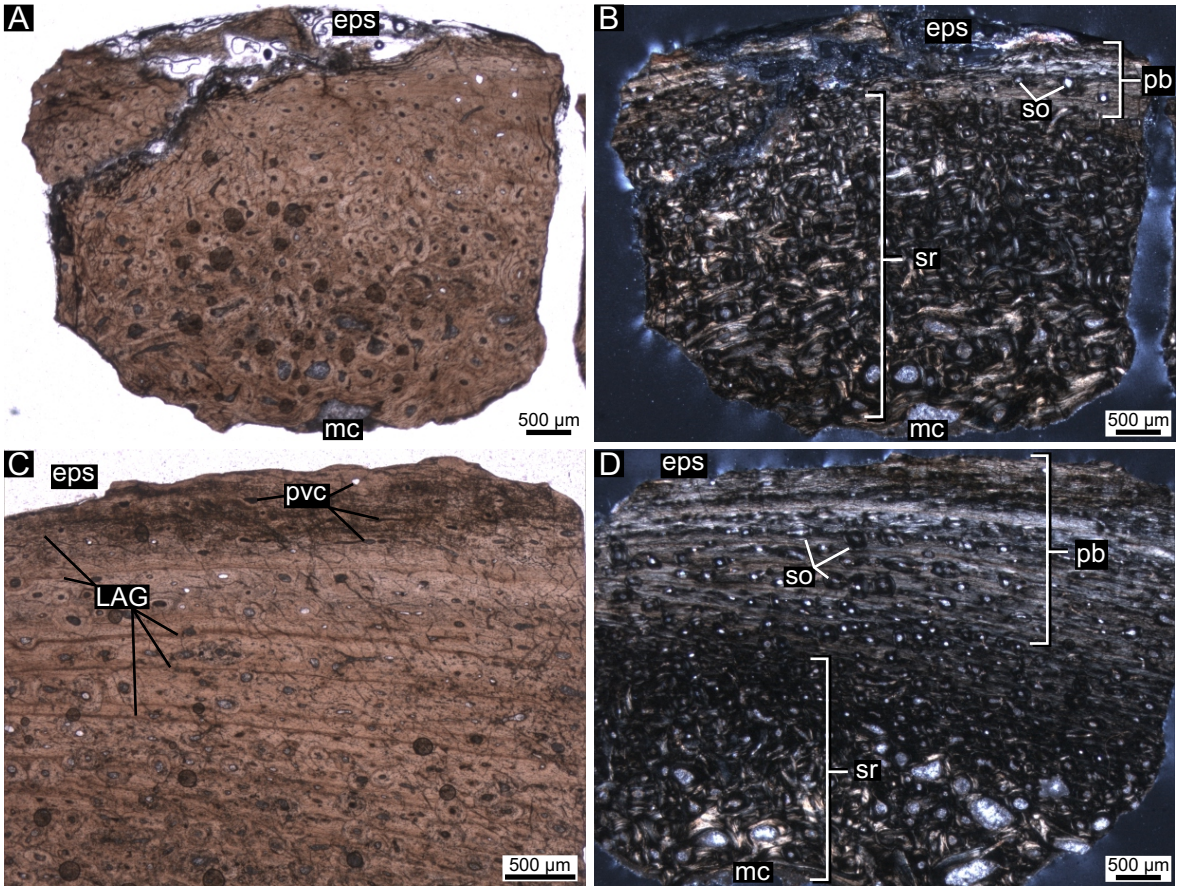

Figure 9. Transverse section of femur R.1382 of *Zalmoxes robustus* representing an intermediate late juvenile-subasdult stage shown under plane (A,C) and crossed plane (B,D) polarizers. **A** and **B**, In this femoral part, strong erosion of the periosteal surface and the extensive secondary remodelling destroyed most of the primary cortex. **C** and **D**, Another cortical part preserves more primary bone and shows several, diversely spaced LAGs, and moderately wide primary canals close to the eroded periosteal surface. Scattered secondary osteons invade the outer cortex.

the presence of a row of sparsely spaced vascular canals at the periosteal surface in R.1608, a new zone seems to have started developing at the time of death (Fig. 10D). This suggests that further but very limited diametrical growth was still possible.

Primary bone is WPC; however, with extremely low woven bone content. Strong diagenetic staining obscures the optical behavior of PFB in both femora, but in clear areas the primary bone shows moderate birefringence that becomes higher along some LAGs (Fig. 10D). The dominance of obliquely and longitudinally cut DO-lacunae in the diagenetically less altered areas of the transverse sections refers to a helical-circumferential PFB.

The histology of the humerus R.6 shows similarities as well as differences compared to that of the femora. A thin layer of endosteal bone rims the medullary cavity. Some erosion cavities invade the cortex in an asymmetrical fashion indicating considerable medullary cavity drift (Fig. 11A). The extent of secondary remodelling is regionally different. In some areas secondary osteons occupy the cortex up to the periosteal surface (Fig. 11C). However, extensive remodelling is generally restricted to the inner half of the cortex, while the outer half is composed mainly of primary bone, and only sparse secondary osteons appear in this area (Fig. 11B).

Porosity of the primary cortex is low with very narrow, predominantly longitudinal vascular canals. However, these vascular canals are still abundant in the inner primary cortical half and become less numerous towards the outer regions. Lamellar infilling is considerable in the primary osteons (Fig. 11B). Up to eight indistinct intracortical LAGs can be counted. Although vascularity decreases considerably, growth marks do not become densely packed in the outermost region, hence no definite EFS can be identified.

Primary bone is WPC, the majority of which in cross section has moderate to high birefringence with lacunar features suggesting helical to circumferential PFB orientation (Fig. 11D). Nodules of woven bone are present between primary vascular canals and are much more frequent in the inner than in the outer cortical regions (Fig. 11C); however their abundance does not appear high enough to refer to this bone tissue as FLC (Prondvai *et al.* 2014a).

Rhabdodon.

1. Early juveniles. The earliest identified juveniles among the *Rhabdodon* specimens are represented by the humeri MHN AIX PV 2001.12.294 (Fig. 12A-D) and MHN AIX PV 2001.65 (Fig. 12E-H). The overall preservation state of 2001.12.294 is very poor. The outermost cortex is strongly eroded, and a meshwork of microcracks and diagenetic staining distort the optical as well as the lacunar features making the inferences on PFB difficult to draw (Fig. 12A,C). Severe cracks also decrease

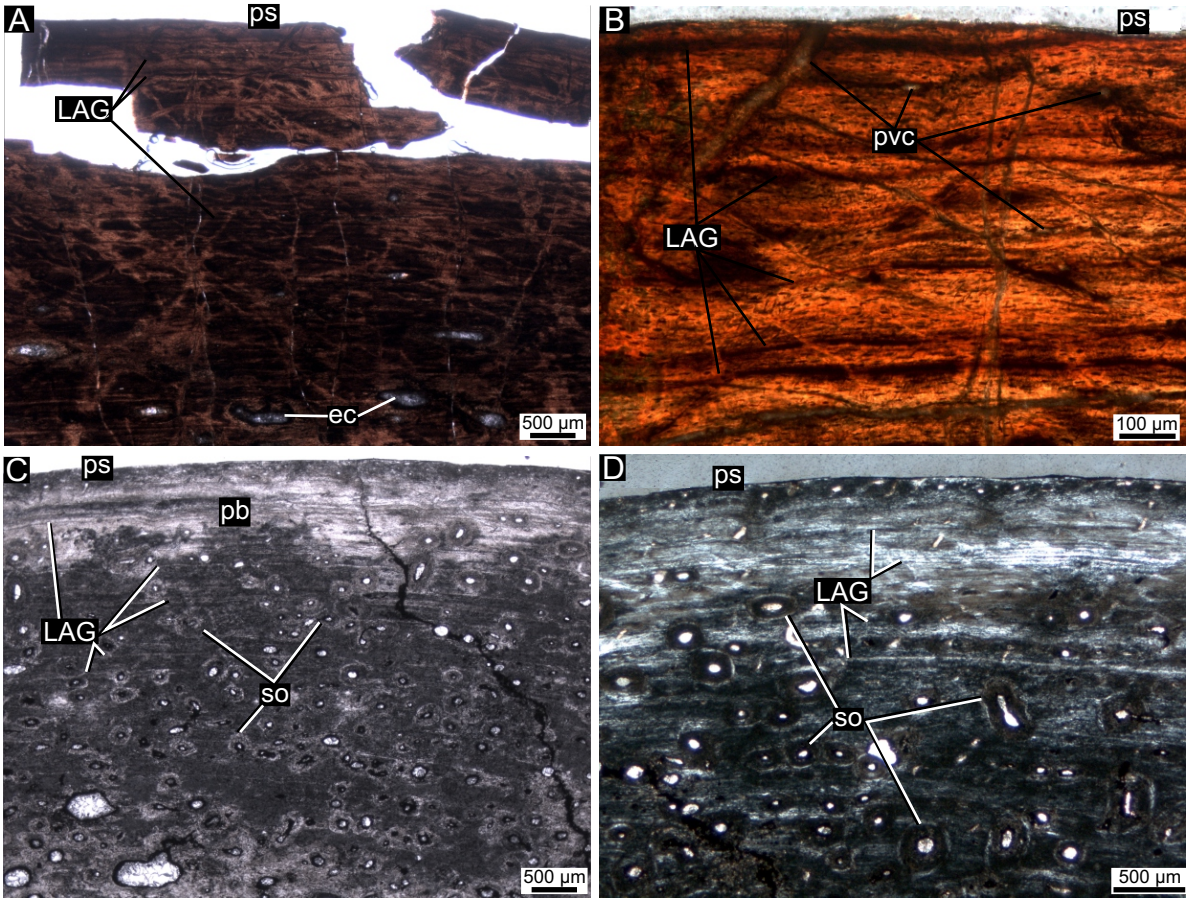

Figure 10. Subadult femora R.1002 of *Zalmoxes robustus* (A,B) and R.1608 of *Zalmoxes shqiperorum* (C,D) in transverse section under single (A,B) and cross (C,D) polarized light. **A**, The broken off outermost periosteal cortex as well as deeper areas with some scattered secondary erosion cavities reveal a high density of LAGs. **B**, Although primary vascular canals still open onto the periosteal surface, these canals are sparse and of very narrow lumen. **C**, Large amount of primary bone is visible but only the outermost layer is void of scattered secondary osteons. **D**, Vascular canals are narrow and sparse, although a circular row of small longitudinal canals rims the periosteal surface.

the visibility of microstructures in 2001.65 (Fig. 12H). Nevertheless, the longitudinal sections (Fig. 12C,D,G,H) are more informative concerning lacunar characteristics, and the combination of the two section planes gives a fairly reliable idea of what the original microstructure of the bones must have been like. The general histology of these humeri is very similar and hence the two specimens are described together; however, wherever observed, differences are highlighted.

The medullary cancellous bone gradually merges into secondary remodelled cortex with secondary osteons of wide lumen, but the outer two-third of the cortex is mostly primary (Fig. 12A,B,H). The primary cortex is densely vascularized, in 2001.12.294 by wide open canals with generally low degree of lamellar infilling (Fig. 12A,C,D). Vascular architecture in cross section is longitudinal with short circumferential anastomoses in 2001.65 (Fig. 12E) and reticular to circumferential in 2001.12.294 (Fig. 12A), but in longitudinal section longitudinal canals clearly predominate in the cortex in both humeri (Fig. 12C,D,H). This suggests a plexiform 3D vascular structure (see Francillon-Vieillot *et al*. 1990; Stein & Prondvai, 2014) in 2001.12.294. In longitudinal section it is clear that the lumen of the longitudinal channels becomes progressively wider peripherally to the extent that they are locally almost as wide as the bony trabeculae surrounding them (Fig. 12C,D). This feature is more prominent in 2001.12.294 suggesting a slightly earlier relative ontogenetic stage for this specimen than for 2001.65. In fact, this high peripheral porosity must have been the most responsible for the attrition of the outermost cortex, and confirms the probably most immature nature of 2001.12.294. There is no architectural change in vascularization towards the periosteal surface in either specimen.

Surprisingly, 8-9 intracortical LAGs can be identified in 2001.12.294, the innermost two of which are more distantly spaced, whereas the rest run closer to each other but they are approximately evenly spaced (Fig. 12B). By contrast three to four growth marks can be detected in 2001.65 but none showed any evident LAG. Hence, cyclical growth in the latter is only detectable based on the longitudinally to helically oriented PFB in the "zones" that is interrupted by a thin layer of more circumferentially oriented PFB of stronger birefringence in cross section (Fig. 12E).

Primary bone tissue is WPC. Where non-lamellated primary matrix seems intact, it has low birefringence in cross section (Fig. 12B,E) with transversely cut DO-derived lacunae. Although in 2001.12.65 it shows strong birefringence along the LAGs, based on the lack of preserved osteocyte lacunae in these regions, it is plausible that diagenetic distortion affected this optical pattern, too (Fig. 12B). However, optical as well as lacunar characteristics in longitudinal section confirm a mainly longitudinally organized PFB in most of the primary cortex in both specimens (Fig. 12D,H). Lacunar preservation in 2001.12.294 is generally low, but clusters of woven bone lacunae are still discernible between adjacent vascular canals (Fig. 12D). Interestingly, in 2001.65, the diagenetic staining seems to have affected mostly the areas of woven bone with SO-lacunae, and it looks as if, due to this staining,

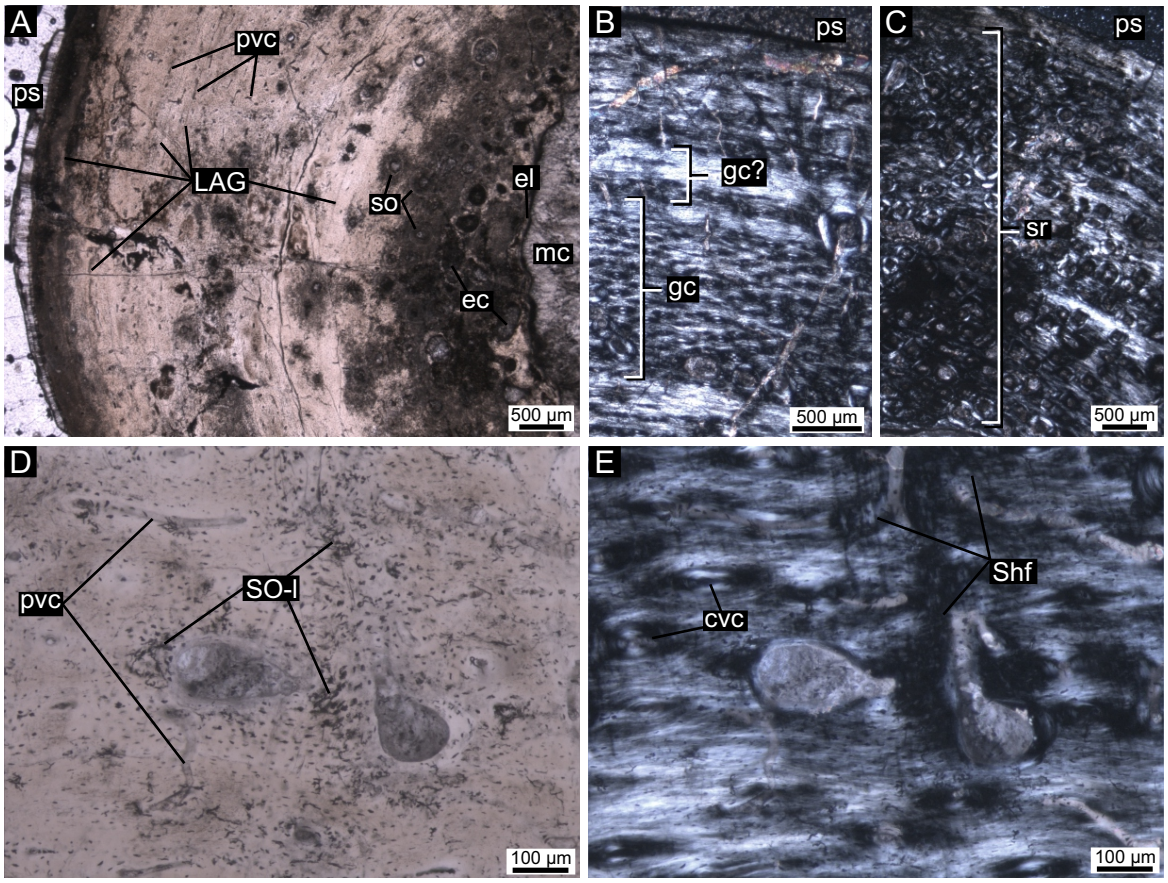

Figure 11. Transverse section of the humerus R.6 of *Zalmoxes* sp. under single (A,C) and crossed plane polarizers (B,D). **A-C**, Several, closely-packed LAGs, indistinct growth cycles in the primary cortex and locally very extensive cortical remodelling characterize the cortex. **D-E**, SO-derived lacunae are present adjacent to the Sharpey's fibres invading the outermost cortex.

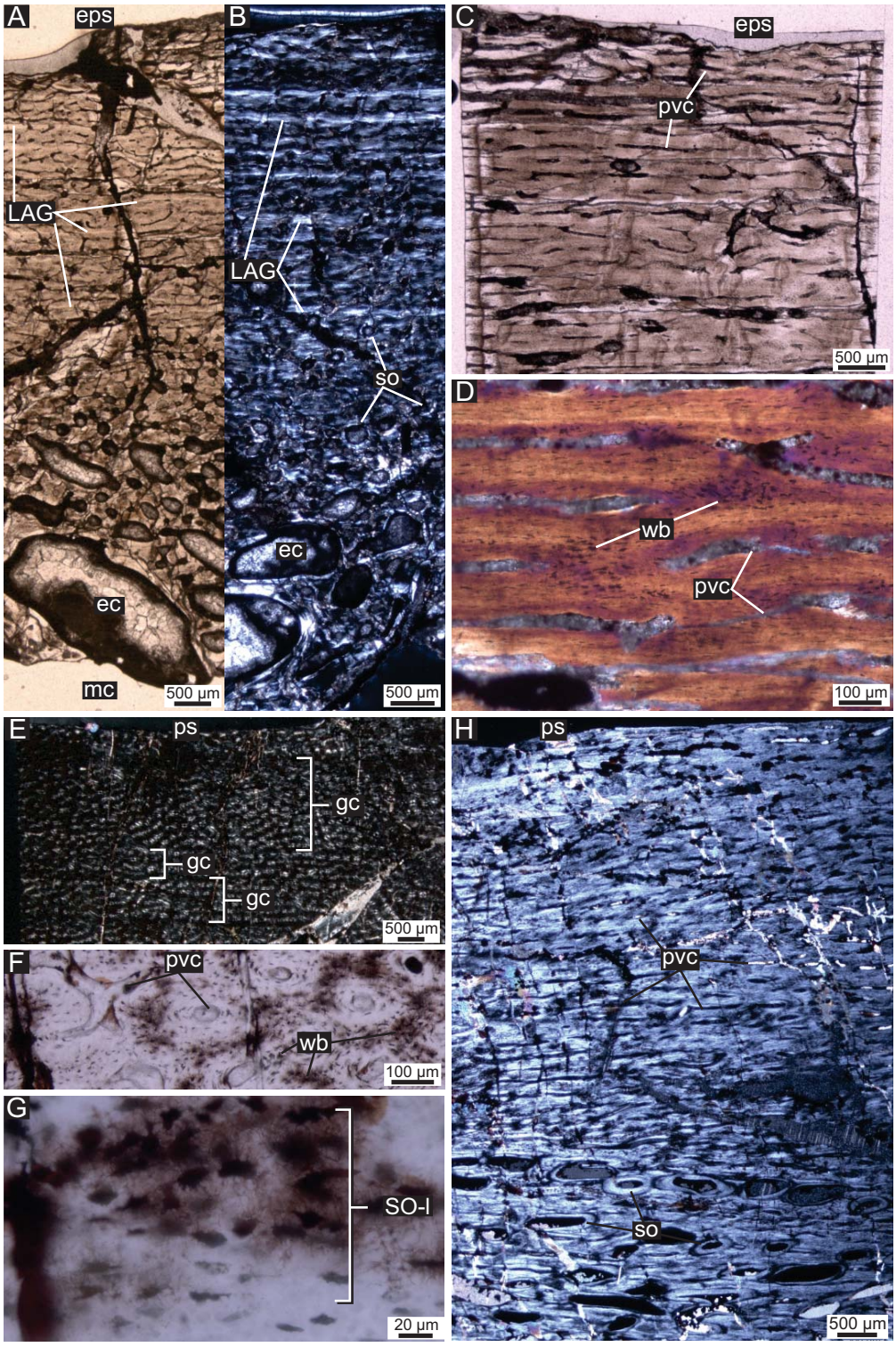

Figure 12. Core samples of early juvenile *Rhabdodon* sp. taken from the humeri MHN AIX PV 2001.12.294 (A-D) and MHN AIX PV 2001.65 (E-H) in transverse (A,B,E,F) and longitudinal (C,D,G,H) sections under plane polarized (A,C,F,G) and cross polarized (B,D,E,H) light aided by λ wave plate in D. **A**, Section through the entire cortex thickness demonstrates the gradual corticomedullary transition with progressively larger erosion cavities among which the smaller ones reach up to the two third of the cortex. The outer cortical third is entirely primary but the periosteal surface is eroded. The abundant, mostly circumferentially running microcracks give the impression of a laminar vascular architecture; however, most vascular canals are longitudinal or short circumferential. Several LAGs are visible with diverse spatial distribution. **B**, Counterslide of the section shown in A. LAGs are rimmed by circumferentially organized parallel-fibred bone appearing bright under cross polarized light. **C** and **D**, Longitudinal section reveals the dominance of longitudinally running vascular canals. Based on the abundance of woven bone nodules adjacent to the wide primary canals the majority of the cortex is defined as fibrolamellar complex. **E**, The prevalent longitudinal vascular architecture is evident in the primary humeral cortex. Very faint growth cycles appear as thin, dark, parallel-running lines rather than LAGs. **F**, Close-up of a primary cortical part with abundant patches of woven bone between primary vascular canals. **G**, High magnification focusing on the lacunocanalicular features of SO-derived lacunae. The improved visibility of the canaliculi in SO-derived lacunae compared to the neighbouring DO-derived lacunae is most probably preservational effect. **H**, The majority of the primary cortex shows up bright in longitudinal section indicating a predominantly longitudinal fibre orientation in the parallel-fibred primary component.

the lacunocanalicular features of woven bone patches had been better preserved than the DO-derived lacunae (Fig. 12F,G). However, the possibility must be taken into account that the stained lacunae may appear larger and more randomly oriented because of the diagenetic alteration and not because of their SO origin. Sharpey's fibres are a decisive structural feature largely influencing the optical and lacunar characteristics of the peripheralmost primary cortex in 2001.65. Despite these difficulties in bone tissue identification originating from preservational effects, the majority of the primary cortex can be defined as FLC.

1. Late juveniles. Five out of eleven sectioned *Rhabdodon* specimens are found to represent late juveniles: the humeri MHN AIX PV 1999.12 (Fig. 13) and MC 472 (Fig. 14A,B), and the femora MC 676 (Fig. 14C-E), MHN AIX PV 2001.113 (Fig. 15A,B), and MHN AIX PV 2001.A3 (Fig. 15C-F). All of these show characteristics of a cyclical but longer period of development with no clear indication of decreasing growth rate. Although not the same skeletal elements, these bones show very similar overall histology, and thus are described together. The only exception is the humerus MC 472 which in some respects shows clear deviations from the rest of the specimens. These differences are highlighted in the descriptions. General preservation state also varies among these specimens with the femora showing an eroded outermost surface, extensive diagenetic staining and/or microcracks obscuring some details of the presumably original structural organization of the bone (Fig. 14C, 15A,C,E).

The border between the cortex and the medullary cavity, where preserved, is not distinct in any of the specimens, because secondary osteons and erosion cavities become progressively larger towards the medulla, and gradually merge into the trabecular system of the medullary cavity (Fig. 13D). Due to weak remodelling, extensive areas of primary bone are still present in the perimedullary regions (Fig. 14C, 15C). This sparse remodelling characterizes only the inner third or maximum half of the cortex except in the humerus MC 472 where it reaches up to the outermost regions leaving only a very thin layer of exclusively primary bone right below the periosteal surface (Fig. 14A,B). Due to the scarcity of secondary osteons, the optical as well as lacunar features of the primary bone in the deeper cortical regions are still discernible in every specimen, and identification is limited only by staining in some cases.

Primary vascular density is comparatively high throughout the cortex with no progressive decrease towards the periosteal surface (Fig. 15A,C), although in most of the femora the outermost cortex is missing. Based on both section planes, the primary vascular canals are mostly longitudinal with shorter circumferential anastomoses defining a poor laminar to plexiform

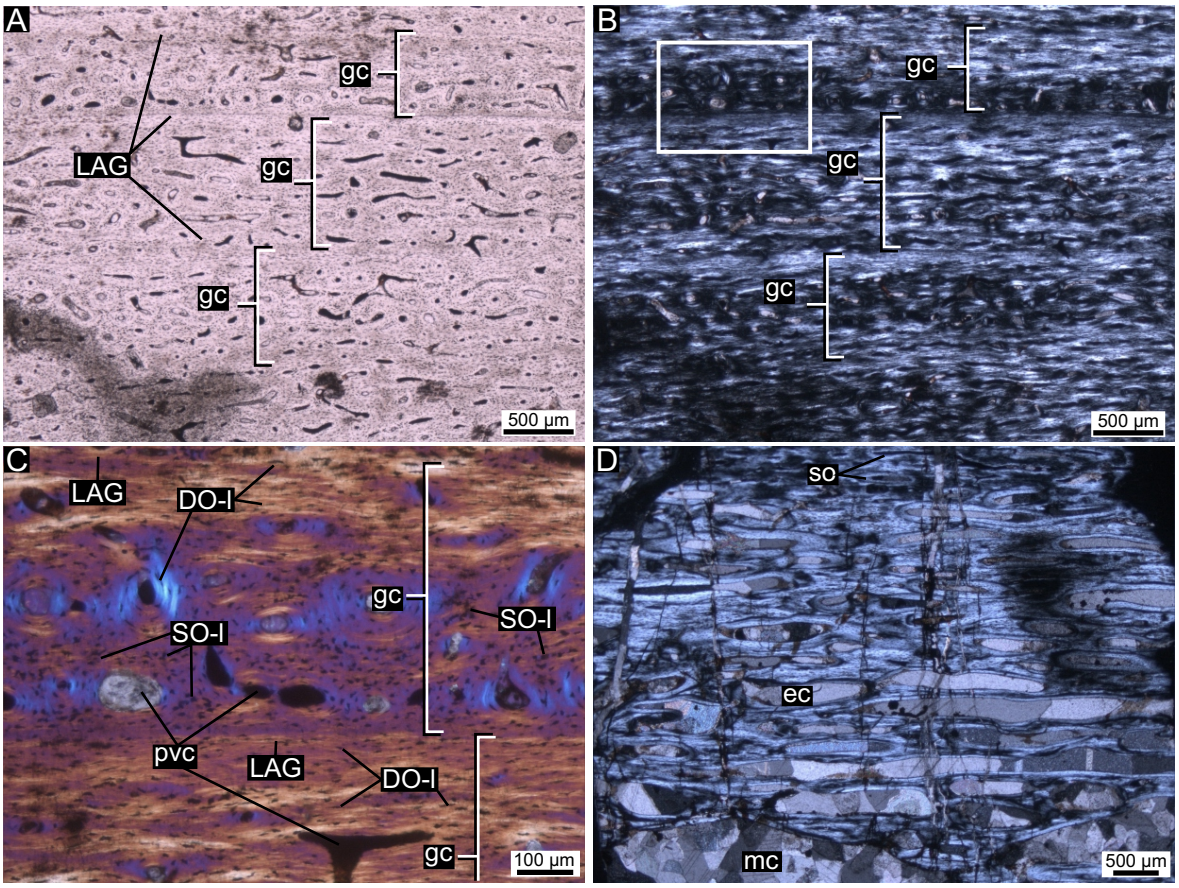

Figure 13. Transverse (A-C) and longitudinal (D) sections of the distal diaphysis of humerus MHN AIX PV 1999.12. **A**, Primary bone in the outer third of the cortex under plane polarized light revealing LAGs and longitudinal to irregular vascular architecture with short circumferential anastomoses. **B**, Same as in A under crossed plane polarizers. White square indicates the magnified area shown in C. **C**, Close-up of the transition between two growth cycles with changing primary structural organization. Note the increasing amount of SO-derived lacunae and longitudinal vascular canals right above the LAG marking the end of the previous growth cycle. A growth cycle closes with a circularly oriented parallel-fibred bone layer. **D**, Longitudinal section of the secondarily remodelled perimedullary cortex with large erosion cavities and longitudinally oriented secondary osteons.

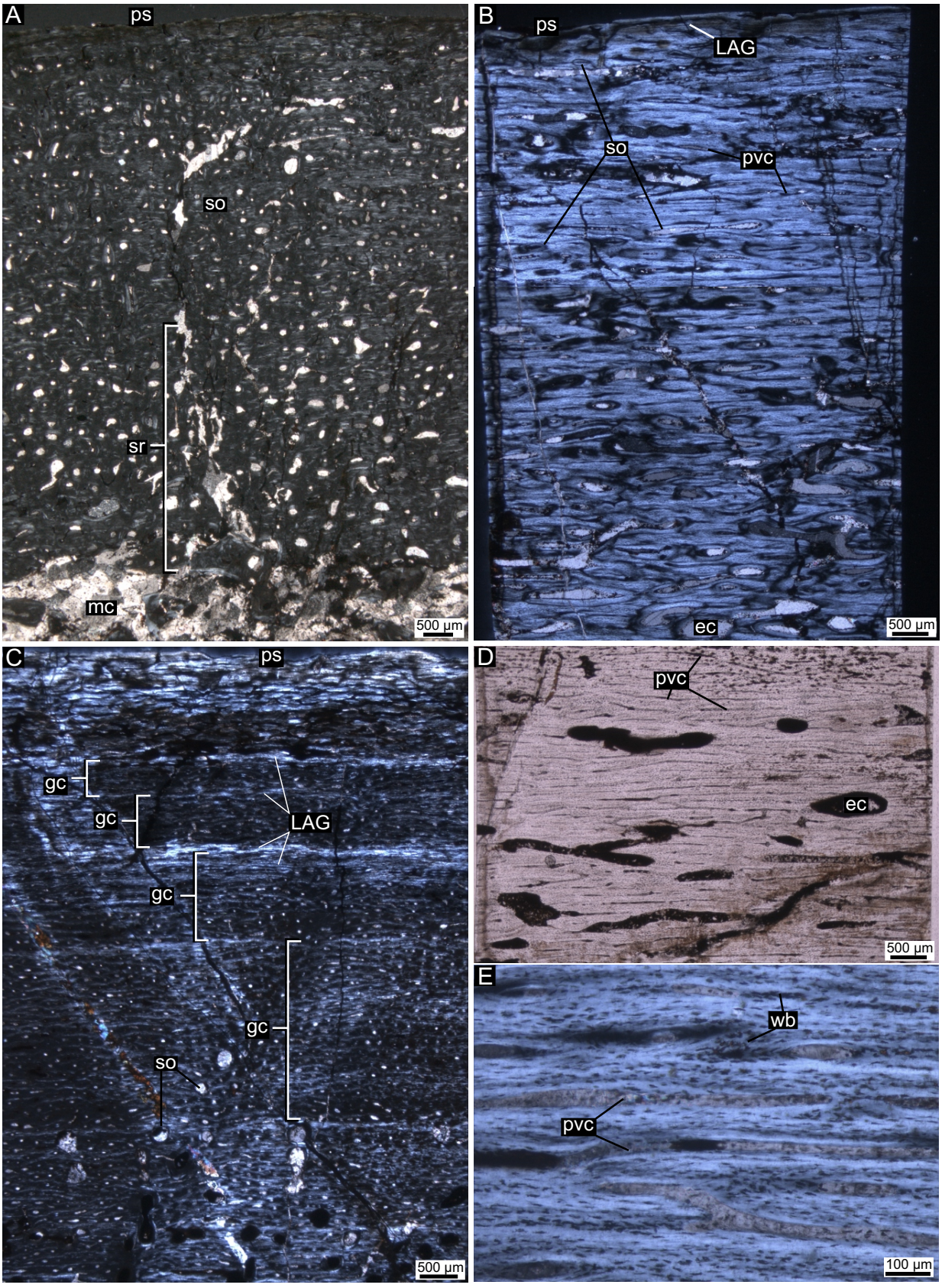

Figure 14. Thin sections of core samples of the Mechin collection 472 humerus (A,B) and 676 femur (C-E). Transverse sections (A,C) and longitudinal sections (B,D,E) under crossed plane polarizers reveal the extent of secondary remodelling and the primary vascular architecture. Whereas secondary remodelling in the humerus (A,B) is more extensive than in the femur (C-E), primary canals run mainly longitudinally in both.

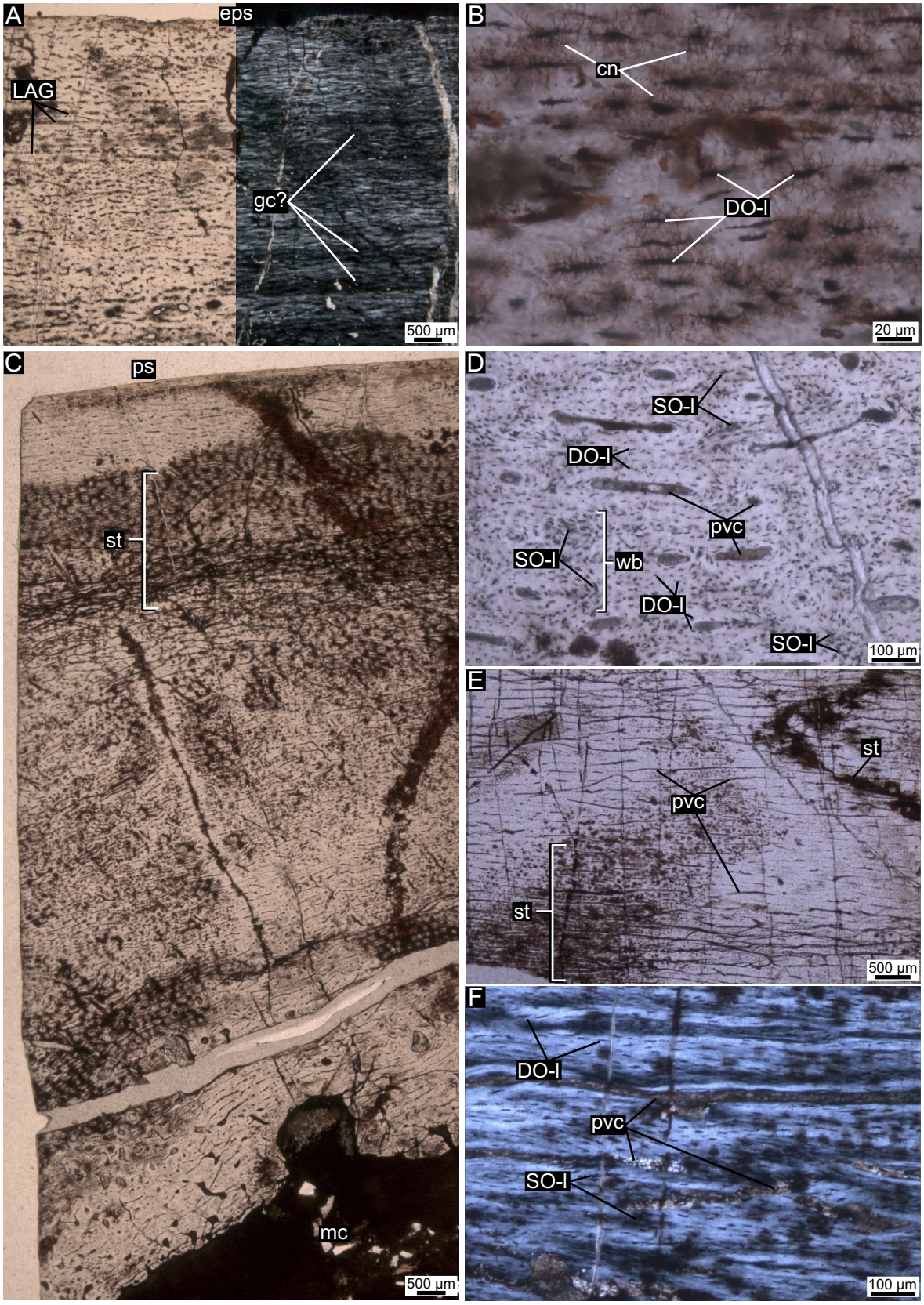

Figure 15. Thin sections of the mid-diaphysis of femora MHN AIX PV 2001.113 (A,B) and 2001.A3 (C-F). **A**, transverse section of the outermost cortex under single and crossed plane polarizers. Note the indistinct miscellaneous growth cycles. **B**, Close-up of the longitudinal section where diagenetic staining seems to improve visibility of finer lacunocanalicular details. **C**, Cross-cortical transverse section under plane polarized light revealing strong staining effects and extensive network of microcracks. **D**, Close-up of the peripheral primary bone area in transverse section under single plane polarizers. Note the abundance of woven bone patches distributed close to the primary vascular canals in the fibrolamellar complex. **E** and **F**, Longitudinal sections under plane polarized (E) and cross polarized (F) light showing the predominantly longitudinal organization of primary bone.

3D vascular architecture (Fig. 14B,C,D, 15C,E). Nevertheless, the humeri MHN AIX PV 1999.2 and MC 472 show more irregularly running transverse canals in cross section (Fig. 13A, 14A). The primary channels are moderately narrow mostly filled up with well-developed lamellae (Fig. 13C, 15D); hence relative cortical porosity is lower in these specimens than in the earlier juvenile humeri MHN AIX PV 2001.12.294 and 2001.65. There is no evident change in vascular architecture towards the periosteal surface except in the femur MHN AIX PV 2001.A3 where a gradual proportional decrease of circumferential canals in favour of longitudinal ones can be detected peripherally (Fig. 15C). Furthermore, in the humerus MC 472, due to the comparatively extensive secondary remodelling, it is difficult to see whether there is any change in vascularity towards the outer cortex, but the vascular canals in the inner two-third of the cortex seem more compacted, i.e., of narrower lumen than the ones in the outer cortical region.

The number of LAGs is very variable among these specimens ranging from one up to ten, and usually more growth marks than definite LAGs can be identified. Growth marks are mostly reflected by cyclical changes in the optical behaviour and/or vascular features of the primary cortex (Fig. 13B,C, 14C, 15A). In the humerus MHN AIX PV 1999.2, only four LAGs out of six growth marks could be counted. By contrast, the humerus MC 472 showed three LAGs in cross section and five in longitudinal section without any obvious structural change in the surrounding primary bone in either section plane. However, this specimen differs from the rest in the greater extent of secondary remodelling that partially may have obscured finer changes in the primary features. Among the femora, all growth marks eventuated in LAGs in MHN AIX PV 2001.A3 and MC 676 with only one and six to eight LAGs, respectively. On the other hand, MHN AIX PV 2001.113 showed seven to ten growth marks that are only very faintly expressed in form of LAGs.

The primary cortex is WPC. In most specimens, the majority of non-lamellar PFB has low to moderate birefringence (Fig. 13B, 14A,C, 15A) with transversely and obliquely cut DO-derived lacunae in cross section (Fig. 13C, 15D), whereas intermediate to strong birefringence (Fig. 14B,E, 15F) with obliquely and longitudinally cut DO-lacunae in longitudinal sections (Fig. 14E, 15B,F). This pattern refers to a helically organized PFB with a dominant longitudinal component. However, PFB being helically organized is a largely generalized statement, because growth marks are reflected in the changing orientation of the structural organization of the primary bone. Cyclicity is manifested in the alternating pattern of longitudinally to helically oriented PFB in the "zones" with more circumferentially oriented PFB of stronger birefringence along the growth marks in cross section (Fig. 13B, 14C, 15A). Lacunar characteristics, wherever they are well preserved, correspond to the optical behaviour of the respective regions.

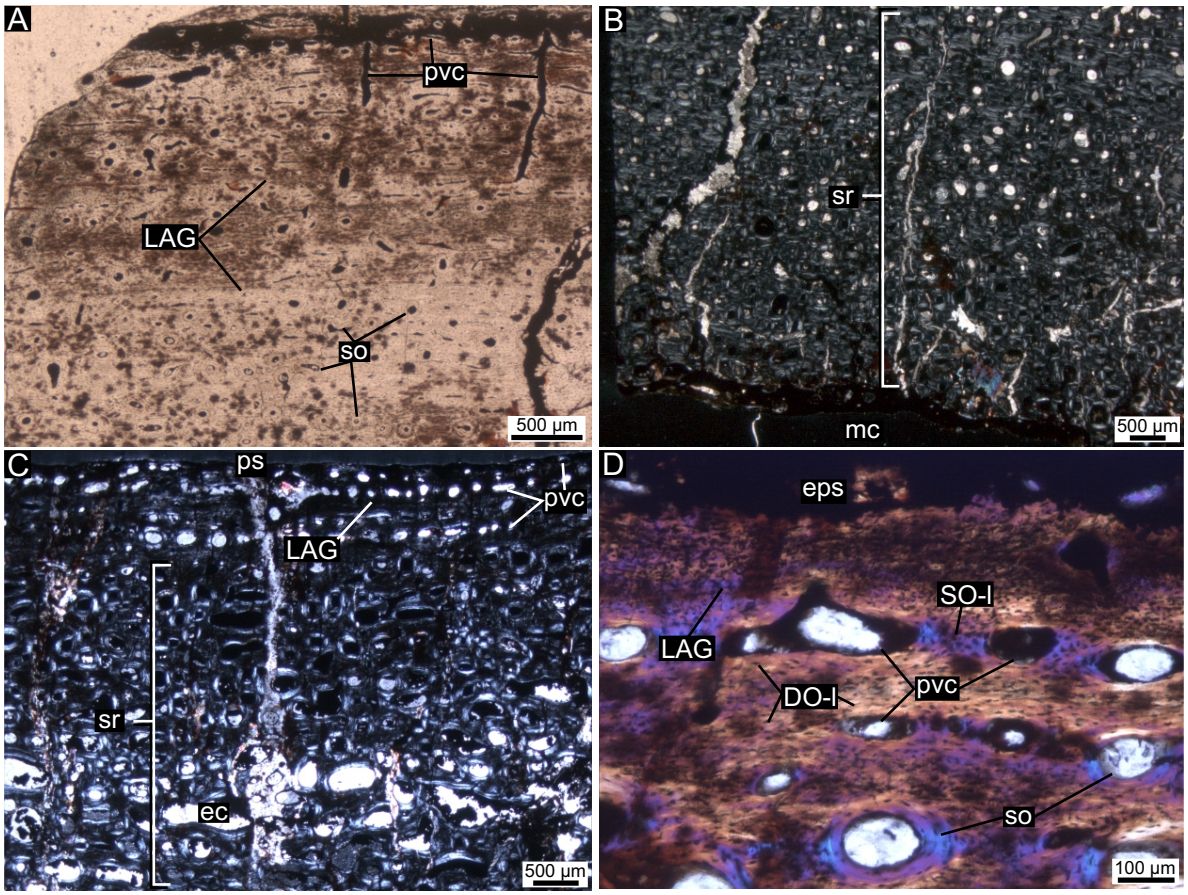

Figure 16. Transverse sections of the mid-diaphyseal (A,B) and distal metaphyseal (C,D) regions of the femur MHN AIX PV 2001.27 under plane (A) and crossed-plane (B-D) polarizers. **A**, The peripheral cortex is densely vascularized by primary canals but secondary osteons also invade this cortical region. **B**, Secondary remodelling obliterates primary structures in the perimedullary cortex. **C**, Secondary remodelling is extensive in the distal metaphysis as well, but primary canals close to the periosteal surface have wider lumen than in the mid-diaphysis. **D**, Close-up of the peripheralmost metaphyseal cortex still containing woven bone with abundant SO-derived lacunae but also some secondary osteons.

Woven bone organized in nodules of five to fifteen SO-derived osteocyte lacunae frequently occurs between and among adjacent vascular canals even in the outermost cortex of each specimen (Fig. 13C, 14E, 15D,F); hence, the primary bone tissue is defined as FLC.

2. Late juvenile – subadult. An intermediate developmental state between the above described late juveniles and the specimen defined as subadult is represented by the femur MHN AIX PV 2001.27 (Fig. 16).

Neither the medullary cavity, nor the outermost cortex is preserved in the thin section of this specimen (Fig. 16D). In addition, strong staining affects most of the primary bone in the peripheral cortical region (Fig. 16A,D). The preserved cortex shows a gradual decrease in the degree of remodelling towards the outer cortex. In this transitional pattern the innermost region is extensively remodelled, thus deep primary tissue can hardly be discerned (Fig. 16B). The middle cortex is moderately remodelled with well distinguishable primary tissue in between, whereas the outermost cortex consists mostly of primary bone with some scattered secondary osteons (Fig. 16A).

The primary vascular canals run mostly longitudinally with short circumferential anastomoses and some thick radial canals (Fig. 16A). Changes in the vascular architecture in the outer cortical third are evident in longitudinal section which shows the increasing ratio of longitudinal canals to the transverse ones towards the periosteal surface. Vascular density is generally moderate but regionally varies, and most primary vascular canals are well-compacted with narrow lumen. The lamellar component of the primary osteon is relatively thin.

Five to eight growth marks are visible in the primary cortex the inner ones of which are very indistinct and the outer ones are strongly distorted due to staining (Fig. 16A). Thus, definite LAGs are hard to identify. Nevertheless, growth marks seem to become more closely spaced in the outer third of the cortex.

The primary cortex is WPC. In cross section, the overall birefringence of non-lamellar PFB is low to moderate with very small but still more elongated than dot-like lacunae indicating that they were obliquely cut in this section plane. Bundles of Sharpey's fibres enter the outermost cortex. In longitudinal section, primary cortex has intermediate to strong birefringence with the DO-derived lacunae being aligned mostly longitudinally to obliquely. Optical and lacunar features in both section planes refer to a longitudinal-helical structural arrangement of the majority of PFB. Woven bone with SO-derived lacunae is present in patches, but difficult to detect due to the staining.

The distal metaphyseal cross section of this specimen, as expected, represents a more actively growing region with primary canals of wide lumen opening onto the periosteal surface (Fig. 16C,D). However, these features are combined with more extensive secondary remodelling than that found in the mid-diaphysis.

3. Subadult. The only specimen among the *Rhabdodon* samples which fits the defined subadult ontogenetic category is the femur MHN AIX PV 2007.4.115 (Fig. 17). Although the core sample went through the entire diaphysis revealing both cortical sides, the bone microstructure of this specimen is very poorly preserved with strong staining and eroded periosteal surface (Fig. 17A,B,C), therefore the information content of its histology is comparatively low.

The medullary cavity is entirely crushed, hence neither its original extent nor its structure can be described (Fig. 17A,B). Although the inner cortical half is secondarily remodelled regionally and scattered secondary osteons can be found even in the outermost cortical region, the cortex is composed predominantly of primary bone.

Primary vascular architecture is predominantly longitudinal with short circumferential anastomoses. Vascular density is relatively high, but porosity is low due to the strong compaction of the primary cavities in which lamellar component is present but not dominant. However, there are a few wide open vascular canals that seem to have been under secondary resorption at the time of death. There is no detectable difference in vascular density or arrangement towards the peripheral cortex, although the outermost layer is most probably strongly eroded.

In transverse section, some LAGs can be traced in the outermost preserved cortex, but poor preservation prevents the correct identification of the number or spacing of those LAGs. In deeper parts of the cortex, LAGs cannot be traced to any extent. On the other hand, two to three and four to five indistinct LAGs can be followed in the peripheral cortex in the longitudinal mid-diaphyseal and the transverse meta-epiphyseal sections, respectively. However, the almost entirely compacted longitudinal vascular canals can give the false impression of LAGs in the longitudinal section.

The majority of the primary non-lamellar bone shows moderate birefringence in transverse section (Fig. 17A), and stronger birefringence in longitudinal section (Fig. 17B) referring to a longitudinal-helical structural organization. However, osteocyte lacuna features are mostly indiscernible due to the poor microstructural preservation state of this specimen, and thus cannot provide additional data on the primary structural organization.

As in the late juvenile – subadult femur MHN AIX PV 2001.27, the meta-epiphyseal sections reveal less mature primary vascular features (Fig. 17D,E) than described for the mid-diaphyseal sections, although with more extensive secondary remodelling (Fig. 17D).

4. Adult. Two, histologically poorly preserved specimens are identified as adults, the femora MHN AIX PV 2007.4.116 (Fig. 18A-D) and MHN AIX PV 2008.1.11 (Fig. 18E-H), although they exhibit fundamentally different microstructural patterns.

The cortex of MHN AIX PV 2007.4.116 is fully remodelled, often by multiple generations of osteons, so that primary bone is completely resorbed (Fig. 18A,D). Secondary osteons are almost completely compacted, and appear mostly dark with a narrow, birefringent outer rim in cross section, whereas they are bright in longitudinal section under crossed plane polarizers. Although lacunar features are generally not preserved, in those small areas where DO-lacunae are present, they are cut transversely in cross section, and along their long axis in longitudinal section supporting the longitudinal organization and thereby tensile nature of the secondary osteons (Ascenzi & Bonucci, 1967, 1968). The extreme cortical remodelling suggests a senescent age for this specimen (Fig. 18A-D).

By contrast, the secondary remodelling front in MHN AIX PV 2008.1.11 only reaches up to the inner half of the cortex, but scattered secondary osteons occur in the outermost region, as well. The innermost cortex is invaded by large erosion cavities, but true medullary trabeculae are not preserved in either of the sections of this specimen (Fig. 18E,F). Primary vascularity is mostly longitudinal with several short circumferential anastomoses (Fig. 18G). Vascular density is relatively high, but porosity is low due to the high compaction degree of the primary vascular canals. Vascular density decreases

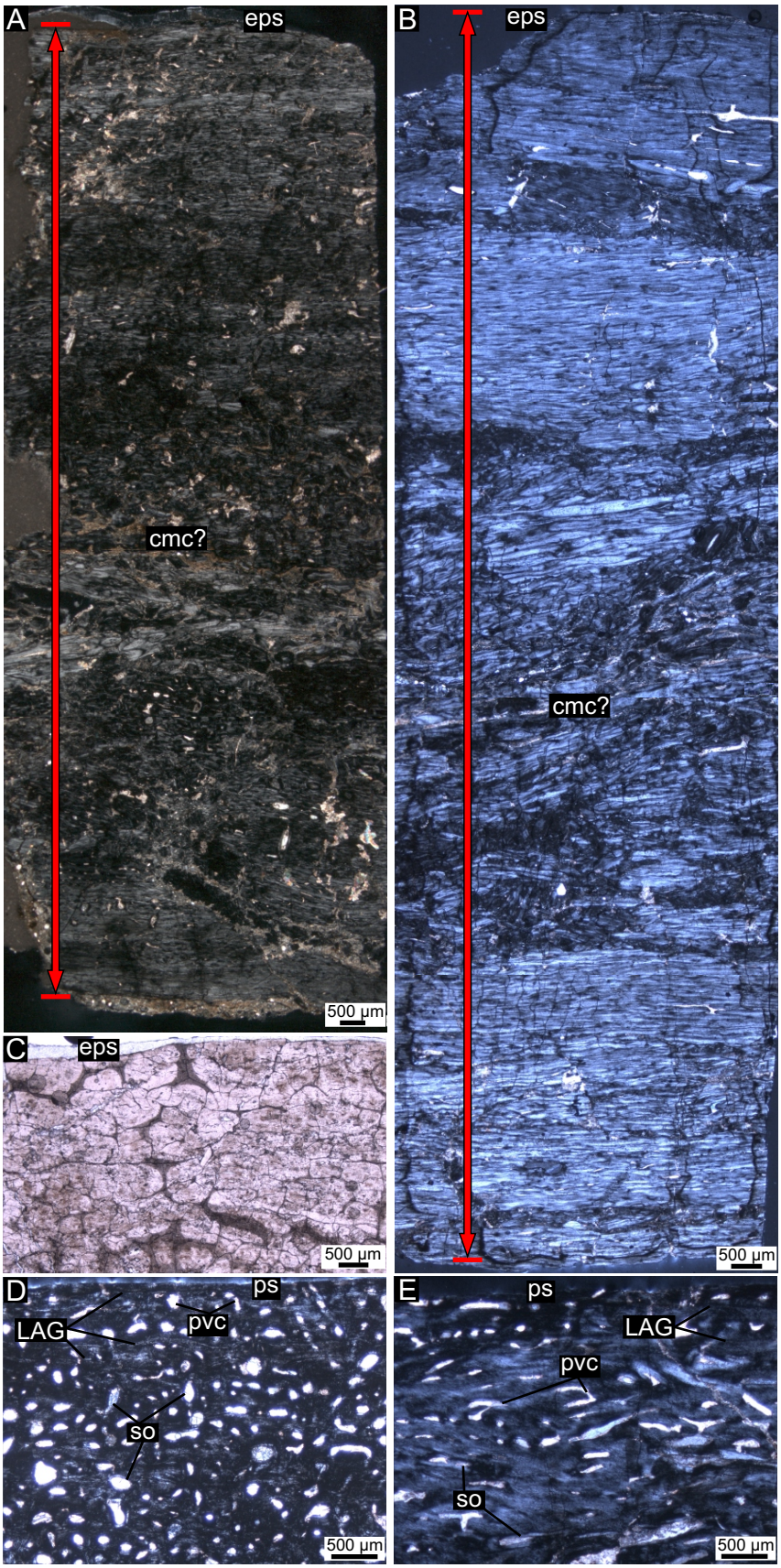

Figure 17. Cross-shaft core samples of the femur MHN AIX PV 2007.4.115. **A** and **B**, Whole mid-diaphyseal core in transverse (A) and longitudinal (B) sections under cross polarized light. The opposing cortical walls crushed and entirely compressed the medullary cavity. Its former location is only recognized by its expected relative position. **C**, Strongly eroded and stained mid-diaphyseal outermost cortex with an extensive network of microcracks under single plane polarizers. **D** and **E**, Meta-epiphyseal transverse (D) and longitudinal (E) sections with wide-open primary vascular canals close to and opening onto the periosteal surface under crossed plane polarizers. Note that secondary osteons are also abundant in the peripheral cortex.

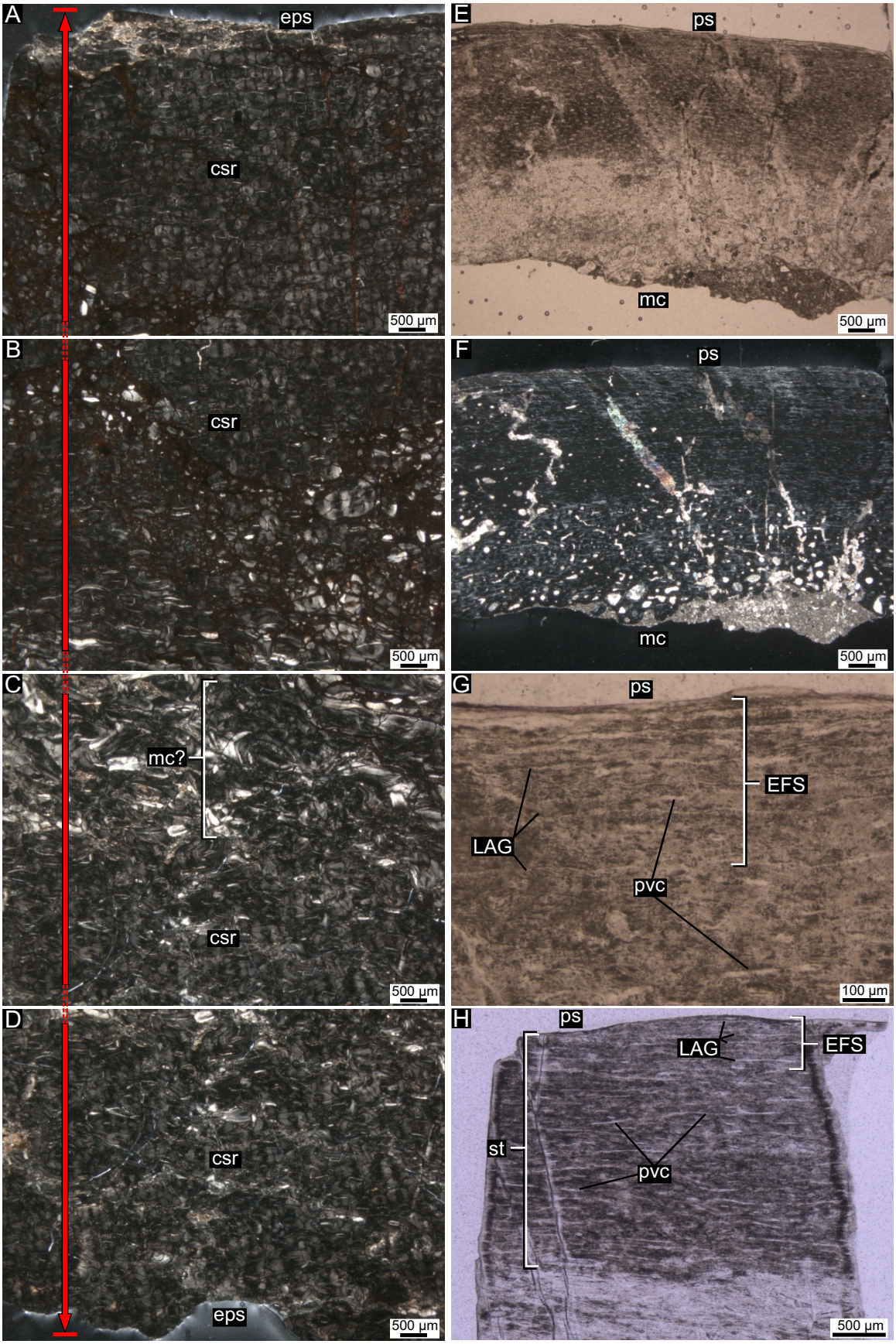

Figure 18. Thin sections of femoral core samples. **A-D**, mid-diaphyseal transverse section of MHN AIX PV 2007.4.116 under cross-polarized light, where individual pictures from A to D lead through the entire bone shaft without representing overlapping regions. Note the strongly eroded periosteal surfaces, the complete secondary remodelling of the cortex, and the almost unrecognizably crushed medullary cavity. **E-H**, mid-diaphyseal transverse sections (E-G) and longitudinal section (H) of MHN AIX PV 2008.1.11 under single plane (E,F,H) and crossed plane (G) polarizers.

towards the periosteal surface in an abrupt fashion. There are three, rather distantly spaced LAGs in the deeper cortex that are followed by six to seven, much more densely packed LAGs in the outermost cortical layer (Fig. 18G). LAGs in the peripheralmost cortex are also clearly detectable in the longitudinal section (Fig. 18H). This area is almost avascular, and along with the characteristic increasing density of LAGs, it most likely represents an EFS. Although bad staining obscures optical as well as lacunar details of most of the primary cortex, stainless areas have high birefringence in longitudinal section with mostly longitudinally or slightly obliquely cut lacunae. Once again, this indicates a mainly longitudinal-helical PFB. Woven bone content is impossible to assess.

DISCUSSION

Implications of the relation between ontogenetic stages and inferred body sizes

The general pattern of the relation between revised ontogenetic stages and inferred body sizes based on reconstructed femur lengths (Fig. 2) suggests some differences in developmental dynamics among the three known genera of Rhabdodontidae.

The almost vertically distributed specimens of the two *Mochlodon* species in the scatterplot (Fig. 2, blue diamonds) show that very different histology-based ontogenetic stages can be represented by the same size range. If the estimated femur lengths are realistic, this distribution pattern indicates high diversity either in achievable adult sizes or in growth dynamics or both among different individuals. Either way, it suggests that size may not be as good indicator of ontogenetic stages in these ornithopods as previously thought and used for other groups (e.g., Horner *et al*. 2009).

Spatial distribution of *Zalmoxes* specimens (Fig. 2, green squares) seems to follow a non-vertical but still very steeply ascending line; however, FGGUB OB 3077, a specimen of uncertain species identity (nr. 16 in Fig. 2), largely distort the appearing trend. In addition, no unquestionably adult specimen has been identified in the sample. Since the relative position of adults in this plot would be of crucial and decisive importance in the qualitative evaluation of the distribution, no further discussion on the course of a potential trend line is possible at present.

Although specimens of *Rhabdodon* are apparently arranged in the expected pattern of proportionally increasing size with progressing histological maturation, the broad size range represented by late juveniles and the single outlier, MHN AIX PV 2008.1.11 (nr. 28, Fig. 2), being an adult with an estimated body size identical to that of adult *Mochlodon* specimens need to be considered. Whereas the diverse sizes of late juveniles can still be explained by the same intraspecific developmental variance as in the case of *Mochlodon*, the large size difference between the adult MHN AIX PV 2008.1.11 and all other *Rhabdodon* specimens, including the early juveniles, is inconsistent with a conspecific origin, and strongly supports a taxonomic distinction of this specimen.

Comparing histology of corresponding elements of rhabdodontids

Comparison of microstructural features of homologous skeletal elements in the context of ontogeny provides more insight into possible taxonomic and/or biomechanical differences. As for differences among these taxa, the phylogenetic relationships (Ősi *et al*. 2012) predict more similarities between *Mochlodon* and *Zalmoxes* than between any of these genera and *Rhabdodon*. However, the same pattern can be the result of biomechanical constraints, because the estimated adult body size of all specimens of *Rhabdodon* except MHN AIX PV 2008.1.11 exceeds that of *Mochlodon* and *Zalmoxes*. Furthermore, respective ontogenetic stages may not represent the same absolute ages, and differences due to this must also be taken into account. Since there was only one scapula and one radius in our sample, and tibiae were available in *Mochlodon* alone, only the humeri and femora of the three rhabdodontid genera can be compared along their developmental trajectories.

Humeri. In total, thin sections of eight humeri were investigated in this study representing all four ontogenetic categories and all three genera, although unfortunately, not a single genus is represented by all ontogenetic stages (Table 1).

The pattern of differences detected in the microanatomy of the corticomedullary border in the humeri speaks for either phylogenetic or biomechanical causes rather than for ontogenetic differences. Whereas there is a smooth transition with medullary trabeculae gradually merging into the cortex in all humeri of *Rhabdodon*, the border between the medullary cavity and the cortex seems more distinct with an endosteal lamellar layer in all humeri of *Zalmoxes* and *Mochlodon* irrespective of their ontogenetic stage.

The proportional distribution of primary and secondary bone in the cortex largely depends on the ontogenetic stage with increasing secondary remodelling as maturation progresses (see e.g., Klein & Sander, 2008; Stein *et al*. 2010), but phylogeny and biomechanics also seem to bear on this feature in the humeri. Although the extent of secondary remodelling varies within one section as well, the pattern is sensibly different between the specimens of *Rhabdodon* and those of *Mochlodon* and *Zalmoxes*. On average, the perimedullary region of the humerus has more compacted resorption cavities and higher density of secondary osteons in *Mochlodon* and *Zalmoxes* than in *Rhabdodon*. Humeri of *Rhabdodon* still have a substantial amount of primary bone preserved adjacent to the medullary cavity even in the late juveniles.

Most aspects of primary vascularity, such as porosity, density and to a certain extent orientation, are strongly dependent on the developmental state of the specimen as discussed above (see Material and Methods). However, specimens of corresponding ontogenetic stages but representing different genera show some consistent differences. The juvenile and late juvenile humeri of *Rhabdodon* are more densely vascularized than the late juvenile humeri of *Zalmoxes*. Furthermore, although the primary cortex is predominated by longitudinal canals in all specimens, among the transverse anastomoses there is a proportionally higher number of short circumferential canals in all humeri of *Rhabdodon* giving the cortex a poor laminar to plexiform vascular architecture, whereas the fewer transverse canals seem to be more randomly oriented in *Mochlodon* and *Zalmoxes*. However, vascular architecture can be regionally different within one section, and different specimens of the same genus show considerable variability in this respect, too. No architectural change in vascularization towards the periosteal cortex could be observed in any of the sections of these humeri; thus, none of these specimens recorded any

potential ontogenetic changes in vascular architecture. This lack of changing pattern is either genuine for the humeri or the transitional cortical parts have not been preserved in any of these specimens. Nevertheless, overall vascular architecture in all humeri is sensibly more irregular than in the femora which have more circularly oriented canals.

The number of growth marks, including LAGs, may vary considerably among corresponding ontogenetic stages even within the same genus, and does not necessarily imply a strong correlation with absolute sizes either. For instance, the histologically least mature humerus MHN AIX PV 2001.12.294 of *Rhabdodon* already shows eight to nine LAGs, whereas all the other *Rhabdodon* humeri of more mature histology exhibit less than seven growth marks and those may not even eventuate in distinct LAGs. In fact, the number of growth marks is also very diverse among the late juvenile humeri of *Rhabdodon* (three to six). By contrast, the number of growth marks in the humeri of *Zalmoxes* is congruent with the recognized ontogenetic stages (4-6 in late juveniles, 8 in the adult), and the single *Mochlodon* humerus, being an adult, also shows a correspondingly high number of LAGs (9). The possible meaning of this difference is discussed below. In all humeri, the spacing of growth marks corresponds to the expected ontogenetic pattern more faithfully than their number does.

The structural organization of the non-lamellar DO-derived primary bone is difficult to generalize, especially due to the considerable differences among specimens in overall preservation state. It is generally true, however, that the orientation of the primary non-lamellar PFB is largely helical the angle of which alternates between more longitudinal and more circumferential following the cyclicity of growth marks. Accordingly, zones usually have a more longitudinal, whereas growth lines and/or annuli a more circular arrangement. Although this pattern is very common among these humeri, the subadult *Zalmoxes* humerus seems to exhibit an overall higher circumferential component in its helical PFB than the rest of the specimens do. The proportional amount of woven bone follows the expected ontogenetic trajectory in each specimen, but it is higher in the late juveniles of *Rhabdodon* than in those of *Zalmoxes*. The lack of humerus of comparable developmental stages in *Mochlodon* prevents further comparisons on the relative amount of SO-derived lacunae.

Femora. Because of their general importance in comparative histological studies (e.g., Sander, 2000; Chinsamy-Turan, 2005; Klein & Sander, 2008), femora were by far the most frequently sampled elements in this study represented by 15 specimens (Table 1). Therefore the ontogenetic series is far more complete in each genus than in the case of the humerus.

Taxonomic and/or ontogenetic patterns in the medullary cavity – cortex transition are difficult to assess due to the generally poor preservation of this region in most of the femoral thin sections. However, this transition appears to be distinct in some specimens, and more gradual in others. The medullary cavity seems relatively distinct from the cortex in all femora of *Mochlodon*, in the late juvenile-subadult femur of *Zalmoxes*, and in the adult MHN AIX PV 2008.1.11 of *Rhabdodon*, whereas the transition is apparently gradual in the early juvenile and subadults of *Zalmoxes*, and in all late juveniles of *Rhabdodon*. The preservation of the remaining specimens does not allow such observations. Thus, the only consistency in this respect is found within the genus *Mochlodon*, while such a congruent pattern could not be shown either in the other genera or among corresponding ontogenetic stages.

The extent and spatial distribution of secondary remodelling seem to be very variable among the femora and show little if any consistency on ontogenetic and taxonomic levels, although the poor preservation of perimedullary regions may obscure important details. Hence, secondary remodelling can be comparatively extensive in early juveniles (in *Mochlodon* and *Zalmoxes*; as opposed to Benton *et al*. 2010) and weaker in subadults (in *Zalmoxes* and *Rhabdodon*), and the expected ontogenetic trend of increasing degree of remodelling with age is not clear in any of the genera, either. Although differences in cutting locations and preservation may account for a large part of this variability, it is possible that these features vary dynamically according to the all-time biomechanical or physiological needs (Currey, 2003).

Besides the expected ontogenetic pattern (see Materials and Methods and Fig. 1A), the primary vascular features of the femora, where not obliterated by resorption and secondary remodelling, also show trends among the three genera. Vascular density of corresponding ontogenetic stages is relatively higher in *Rhabdodon* than in *Mochlodon* and *Zalmoxes*. Although the vascular architecture of every specimen is clearly dominated by longitudinal canals, relatively more circumferential anastomoses are present in the femora of *Rhabdodon* than in those of *Mochlodon* and *Zalmoxes* in all ontogenetic stages.

Growth marks may be variably expressed even within a single specimen: it may eventuate in LAGs alone referring to sudden interruptions in growth, or in annuli with or without LAGs representing a longer period of slow growth. The number of LAGs and/or growth marks seems to correspond well with the respective ontogenetic stages in *Mochlodon* (2 and 5-6 in the early and late juvenile, respectively, 5 in the subadult, 14 in the adult) and *Zalmoxes* (0 in the early juvenile, 10-12 in the late juvenile-subadult, 13-17 in the subadults), but less so in those *Rhabdodon* femora where complete secondary remodelling did not prevent the counting (1-10 in late juveniles, 5-8 in the late juvenile-subadult, 0-3 in the subadult, 9-10 in the adult). Furthermore, growth marks mostly appear as LAGs in the femora of *Mochlodon* and *Zalmoxes*, whereas they are less frequently marked by LAGs in *Rhabdodon*.

Structural orientation of the primary bone in the femora seems to follow largely the same pattern as in the humeri with helical orientation in the zones and more circumferential arrangement along LAGs and in the annuli. Although obliterated in many cases, the relative amount of SO-lacunae in corresponding ontogenetic stages seems to be the lowest in *Mochlodon*, but in later ontogenetic stages it becomes very low in both *Mochlodon* and *Zalmoxes* as compared to *Rhabdodon*.

Comparing histology of rhabdodontids with that of other ornithopods

Bone histological descriptions and illustrations of several mid-diaphyseal transverse sections have been published on other ornithopods, namely *Dysalotosaurus* (Chinsamy, 1995; Hübner, 2012), *Hypacrosaurus* (Horner *et al*. 1999), *Maiasaura* (Horner *et al*. 2000), *Orodromeus*, *Dryosaurus*, *Tenontosaurus*, *Camptosaurus* (Horner *et al*. 2009; Werning, 2012), and undetermined basal ornithopods ("hypsilophodontids") from polar regions (Chinsamy *et al*. 1998; Woodward *et al*. 2011). Based on the descriptions and depictions provided in these studies, gross comparisons of the humeral and femoral bone

histology between these ornithopods and the rhabdodontids are possible. Figure 19 shows the simplified phylogenetic interrelationships of the considered taxa (based on Ősi *et al*. 2012 and McDonald, 2012) to provide a phylogenetic framework for these comparisons.

Humeri. Humeral histology has only been investigated in *Maiasaura* (Horner *et al*. 2000), *Dysalotosaurus* (Hübner, 2012) and *Tenontosaurus* (Werning, 2012); however, specific histological description of the humerus was only provided for *Dysalotosaurus* (Hübner, 2012) and *Tenontosaurus* (Werning, 2012).

Although the structural appearance of both, the medullary cavity and the region between the medulla and the cortex, is strongly preservation-dependent, a distinct corticomedullary border seems to characterize the mid-shaft region in *Dysalotosaurus*, whereas a more transitional microanatomy is found in the humeri of *Tenontosaurus*. From late juveniles to adults, the long bones of *Maiasaura*, presumably including the humerus, have been described to exhibit an extensive medullary trabecular system with the adults showing a relatively larger medullary cavity than the subadults. The condition described in *Dysalotosaurus* is similar to that found in *Mochlodon* and *Zalmoxes*, whereas *Tenontosaurus* and probably *Maiasaura* resemble *Rhabdodon* in this respect. This distribution apparently corresponds with the differences in body sizes with *Mochlodon*, *Zalmoxes*, and *Dysalotosaurus* representing the smaller and *Rhabdodon*, *Tenontosaurus*, and *Maiasaura* the larger size categories.

Secondary remodelling is limited to a few secondary osteons even in more mature specimens of *Dysalotosaurus*, whereas it becomes progressively more extensive and dense with maturation in *Tenontosaurus* reaching up to the middle cortex in specimens identified as adults. Secondary remodelling in the long bones of *Maiasaura* is reported to start already in late juveniles, but in the humerus of the adults secondary osteons are densely packed in the internal cortex and diffuse and uniformly spread in the external cortex. The negligible secondary remodelling reported for *Dysalotosaurus* does not correspond to the condition found in all rhabdodontids, where the extent of remodelling is considerable even in juveniles and the difference among the three genera lies mainly in the density of secondary osteons. *Tenontosaurus* and adult *Maiasaura*, on the other hand, exhibit a pattern of remodelling reminiscent of that observed in rhabdodontids. Because of the lack of corresponding ontogenetic ages, further comparison of this ontogeny-dependent feature between *Tenontosaurus* and the three rhabdodontid genera is not possible at present.

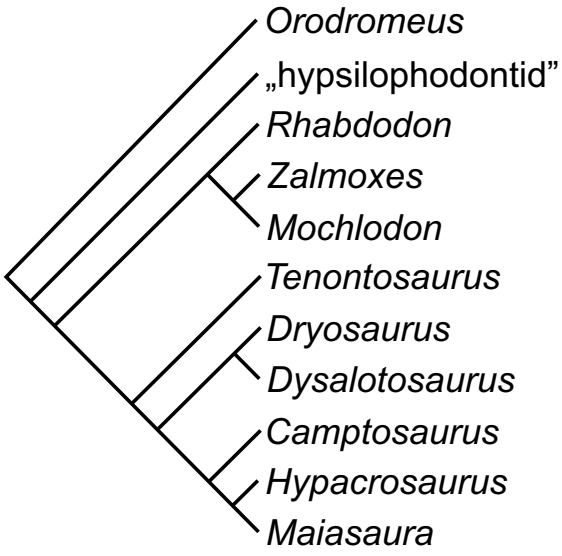

Figure 19. Simplified phylogenetic interrelationships of the ornithopod taxa used in the comparative histological investigation. Phylogenetic position of the non-hadrosauriform and hadrosauriform ornithopods is based on Ősi *et al*. 2012 and McDonald, 2012, respectively.

Primary vascular architecture is plexiform to reticular in juveniles and more laminar in more mature specimens of *Dysalotosaurus* with abundant longitudinal canals, whereas mostly longitudinally running canals organized in circumferential rows are found in *Tenontosaurus* with some short circumferential anastomoses in larger specimens. In both genera, the density of vascular canals is high. These features in *Maiasaura* are once again generalized to long bones where the detectable ontogenetic pattern ranges from all kinds of vascular architectures in late juveniles to a plexiform and laminar arrangement in subadults and adults. As in the pattern of remodelling, primary vascular architecture in the humeri of *Tenontosaurus* is more similar to that found in the humeri of rhabdodontids which do not develop laminarity as seen in *Dysalotosaurus* and apparently *Maiasaura*. In particular, vascular features of *Tenontosaurus* resemble those of *Rhabdodon* the most, whereas *Mochlodon* and *Zalmoxes* have lower vascular densities and less circumferential anastomoses.

Growth marks in *Dysalotosaurus* and in the late juveniles of *Maiasaura* do not always eventuate in LAGs, and can be very indistinct. Annuli are mostly distinguished based on the presence of circularly oriented vascular canals and primary parallel-fibred bone. By contrast, *Tenontosaurus* humeri reveal distinct LAGs in the growth cycles. In *Dysalotosaurus* and *Tenontosaurus*, the number of growth marks seems to correspond to the skeletal maturity of the specimen, whereas five LAGs were reported in the subadult and only three in the adult humeri of *Maiasaura* showing less consistency with the assigned ontogenetic stage. However, this inconsistency may be the result of expansion of the medullary cavity at adult stage (Horner *et al*. 2000) that could have eroded the innermost LAGs. Interestingly, *Dysalotosaurus* and the late juveniles of *Maiasaura* resemble *Rhabdodon* in having indistinct growth marks, while the pattern described for the *Tenontosaurus* humeri with clear LAGs is more reminiscent to that found in *Mochlodon* and *Zalmoxes*. Regarding the number of growth marks, the condition described for *Dysalotosaurus* and *Tenontosaurus* is similar to that found in *Mochlodon* and *Zalmoxes*, whereas the little correspondence between the number of growth marks and relative skeletal maturity in *Rhabdodon* might have characterized the humeri of *Maiasaura* as well.

The majority of the primary bone tissue is referred to as “fibro-lamellar” (*sensu* Ricqlès, 1975, Francillon-Vieillot *et al*. 1990) in all of these ornithopods, although the gradually changing character of primary bone from woven to FLC to PFB during development has been emphasized in *Tenontosaurus* (Werning, 2012), which again implies the increasing proportion of PFB in the primary bone along the developmental trajectory. However, overall structural organization of the humeral primary parallel-fibred bone is not described in either *Dysalotosaurus* or *Tenontosaurus*, and the figures showing histological features of the humeri provided in these studies do

not show high enough magnification for the reader to judge. Nevertheless, the externalmost cortex of subadult and adult *Maiasaura* long bones is described as longitudinally organized parallel-fibred periosteal bone.

Femora. Femoral microstructure of all ornithopod genera mentioned above has been described (Chinsamy, 1995; Chinsamy *et al*. 1998; Horner *et al*. 1999; Horner *et al*. 2000; Horner *et al*. 2009; Woodward *et al*. 2011; Hübner, 2012; Werning, 2012).

All cited ornithopod genera seem to possess a distinct corticomedullary boundary and, at least in more mature specimens, an evident endosteal layer surrounding the medullary cavity of the femur. Except for *Maiasaura* and *Hypacrosaurus*, the femoral medullary cavity in these animals appears to exhibit little spongiosa. Since the microanatomy of this region in the femur is mostly poorly preserved and does not show unambiguous generic tendency among rhabdodontids, further interspecific comparison of this feature is not attempted here.

The degree of secondary remodelling increases with skeletal maturation in *Dysalotosaurus*, *Tenontosaurus* and *Maiasaura*, whereas very week secondary remodelling seems to characterize the femur of *Orodromeus*, *Dryosaurus*, and the undetermined polar "hypsilophodontid" at later stages of development as well. In the single adult specimen of *Hypacrosaurus* dense Haversian tissue invades the outer cortex but not as extensively as the internal cortex where almost no primary structures are visible. The single juvenile specimen of *Camptosaurus* does not show evidence of remodelling. This histological feature has proven to be very diverse in rhabdodontids with neither taxonomic nor ontogenetic trends to be detected, and thus cannot be used to compare rhabdodontids with the other mentioned ornithopod genera.

Primary vascular architecture in the femur is increasingly laminar with maturation in *Dysalotosaurus*, *Dryosaurus*, *Maiasaura*, and apparently in *Hypacrosaurus*, mostly reticular or plexiform in *Orodromeus* and in the undetermined polar "hypsilophodontid", and mostly longitudinal with some circumferential or irregular anastomoses in *Tenontosaurus* and *Camptosaurus*. In this respect, rhabdodontids show more similarities to the latter two taxa; however, some larger femoral specimens of *Rhabdodon* locally exhibit a plexiform vascular arrangement. This feature does not seem to follow trends in body size or phylogenetic relations of these genera.

As in the humerus, superimposed concentric growth cycles resulting from slight modulation in vascular characteristics and sometimes independently from LAGs are found in the femoral cortex of *Dysalotosaurus*, *Hypacrosaurus*, in the late juveniles of *Maiasaura*, and in the indeterminate polar "hypsilophodontid". Presence of such growth cycles without development of distinct LAGs characterizes *Rhabdodon* as well; however, unlike in *Rhabdodon*, the number of LAGs and other growth cycles seem to follow the expected increase corresponding to ontogenetic maturation in all described ornithopod genera. Growth marks are observable already in the late juveniles of *Dysalotosaurus*, *Maiasaura*, in the indeterminate "hypsilophodontid", and most probably in *Hypacrosaurus*, whereas they start to appear only in subadults in *Orodromeus*, *Dryosaurus*, and *Tenontosaurus*. There is no LAG or other growth mark in the single juvenile specimen of *Camptosaurus*. The early appearance of growth cycles is also characteristic to all rhabdodontid genera.

Primary femoral cortex was described as FLC in most cases, although with clear specification of changing proportions of woven and parallel-fibred bone during ontogeny. Except for a brief mention of longitudinally organized parallel-fibred bone in the outer cortex of subadult and adult femora of *Maiasaura* and *Hypacrosaurus*, the orientation of the bulk of primary parallel-fibred bone is not considered or demonstrated in detail in any of these ornithopod taxa; probably for the same reason as discussed in the case of the humeri.

Taxon-specific patterns and their implications

Finding taxon-specific patterns (i.e., common features as well as consistent differences) in the ontogenetic histology of any fossil group of vertebrates would be of two obvious advantages. First, the evolutionary appearance and phylogenetic distribution of these taxon-specific characters or character combinations could be analysed. Second, such taxon-specific histology would have the potential to be used as an accessory tool for taxon identification in case of elements of dubious origin. Bone histology of the investigated elements of the three rhabdodontid genera appears to show some consistent pattern at family as well as generic levels. For instance, a common feature found in all rhabdodontid elements is the relatively early onset of cyclical growth and secondary remodelling during skeletal development. This combined early appearance seems to characterize the bones of the distantly related, derived ornithopod genus, *Maiasaura* (Horner *et al*. 2000), and possibly *Hypacrosaurus* as well (Horner *et al*. 1999). The most frequent pattern among basal ornithopods is the early onset of cyclical growth but later onset of secondary remodelling, such as in *Dysalotosaurus* (Chinsamy, 1995; Hübner, 2012), *Orodromeus* (Horner *et al*. 2009), and in the undetermined polar "hypsilophodontids" (Chinsamy *et al*. 1998; Woodward *et al*. 2012). By contrast, visible growth marks and secondary osteons first appear in the subadult ontogenetic stage in *Dryosaurus*, *Tenontosaurus*, and most likely in *Camptosaurus* (Horner *et al*. 2009; Werning, 2012). This phylogenetic distribution speaks for an independent acquisition of the similar developmental timing of the onset of these histological characters in the basal rhabdodontid and derived hadrosaurid groups. In the context of adult body sizes, no tendency seems to correspond to the timing of character combinations demonstrated among the different ornithopods, because the same pattern occurs among animals with broad body size ranges (e.g., *Mochlodon* ~22 cm vs. *Maiasaura* ~100 cm adult femur length), whereas different patterns are also found among genera with similar body sizes (e.g., *Dysalotosaurus* and *Zalmoxes*). Furthermore, as opposed to all other ornithopod genera, there seems to be no clear positive relationship between the extent of secondary remodelling and skeletal maturation state at least in the femora of any of the rhabdodontids. Nevertheless, the underlying factors influencing the formation and spatial distribution of growth marks and secondary remodelling are controversial. For instance, growth interruptions resulting in LAGs in the bone tissues are widely accepted to reflect annual cyclicity (e.g., Castanet *et al*. 1993; Buffrénil & Castanet, 2000; Matsuki & Matsui, 2009; Köhler *et al*. 2012); however, a number of studies showed that several reasons may cause deviations from a one-to-one correspondence between the number of growth lines and years of age (Esteban *et al*. 1996; Björndal *et al*. 1998; Horner *et al*. 1999, 2000; Buffrénil & Castanet, 2000; Jakob *et al*. 2002; Klein *et al*. 2009). As for bone remodelling, it has an extremely complex regulatory system (Javed *et al*. 2010; Crockett *et al*. 2011) and is explained by several functional factors, such as biomechanical competence, cell death, bone

aging and microfracture-repair, calcium and phosphate storage for mineral homeostasis, and grain change (see Currey, 2003 and references therein), while it also maintains a constant bone mass (Frost, 1969). However, none of these functional factors gives adequate explanation for the trigger of the ontogenetically early onset of remodelling (e.g., in humans) or the generally more intense remodelling in the perimedullary cortical areas of long bones (Currey, 2003); a pattern that is evident in our rhabdodontids, as well. This suggests a mostly neglected, maybe non-functional factor resulting in genetically largely predetermined distribution of secondary remodelling, via hormonal and hypothalamic control (Amling *et al*. 2000; Pogoda *et al*. 2005), that might show a phylogenetically constrained distribution. Our current knowledge on the fine-scale regulation of both development of growth marks and secondary remodelling in bone tissues is seemingly quite limited; hence the potential phylogenetic and/or functional significance of this pattern in rhabdodontids cannot be inferred at present.

Genus-specific differences also seem to occur among the three rhabdodontid genera. *Mochlodon*, for instance, seems to differ from both *Zalmoxes* and *Rhabdodon* in having relatively thinner long bone cortices at earlier ontogenetic stages and less trabeculae in the medullary cavities than found in the limb bones of the latter two genera. On the other hand, long bones of *Rhabdodon* are more densely vascularized with relatively higher woven bone content than those of *Mochlodon* and *Zalmoxes* at any corresponding ontogenetic stages. These latter characteristics define primary bone as FLC in most *Rhabdodon* specimens, whereas FLC, as defined by Prondvai *et al*. (2014a), only occurs in the earliest ontogenetic representatives of *Mochlodon* and *Zalmoxes*. This indicates a prolonged rapid growth phase in *Rhabdodon* when compared to *Mochlodon* and *Zalmoxes*. Furthermore, the number of LAGs and other growth marks in *Rhabdodon* is often inconsistent with the ontogenetic stages indicated by other histological features, whereas *Mochlodon* and *Zalmoxes* show increasing number of growth lines with increasing histological maturation. Apart from *Rhabdodon*, the only ornithopod where reported LAG count, at least in its humerus, seems not to reflect the ontogenetic stage is *Maiasaura* (Horner *et al*. 2000). However, it must be noted that, unlike in rhabdodontids, the ontogenetic assignment of the other histologically investigated ornithopod taxa was strongly influenced, if not entirely based on, the absolute size of the specimens rather than on the skeletal maturity state. Hence, the revealed correspondence between the number of growth marks and inferred ontogenetic stages can simply be a positive relationship between the number of growth marks and size (rather than histological developmental state) of the specimens.

Even so, the large variability in the number of LAGs and other growth marks among corresponding ontogenetic stages in *Rhabdodon* is still an interesting, and seemingly unique feature of this genus and may have further implications. On the one hand, it may refer to high degree of plasticity in growth trajectories that was expressed by a less determined and controlled cyclicity of growth in *Rhabdodon* than in *Zalmoxes* and *Mochlodon*. This pattern can be interpreted as a temporal decoupling of predetermined cyclical growth interruptions from the different phases of the growth trajectory (Fig. 1) enabling individually different reaction norms (Schmalhausen, 1949) in growth dynamics. Such decoupling could have made way for reaching larger body sizes when no other restricting factor was present. Hence, it could have been a key heterochronic developmental "tool" canalized by the adaptive value of greater body sizes in the evolutionary process of autapomorph giantism, as the latter phenomenon was suggested for this genus based on the numerical analysis of body size evolution in basal ornithopod taxa (Ősi *et al*. 2012). However, it is also conceivable that the more regular growth cycles observed in *Mochlodon* and *Zalmoxes* reflect a long-term predictable environment with stable selection pressures, whereas the irregularities found in *Rhabdodon* refer to a less stable habitat with ever changing ecological challenges.

On the other hand, inconsistencies between growth mark counts and ontogenetic stages may imply taxonomic differences in the *Rhabdodon* sample. This hypothesis is supported at least in the case of one specimen, the femur MHN AIX PV 2008.1.11, where substantial evidence indicates its different taxonomic status from the rest of the investigated specimens of *Rhabdodon*. First, the relationship between histology based ontogenetic stages and inferred body sizes of all other specimens still fits the reasonable range of intraspecific variability, whereas the adult status of the femur MHN AIX PV 2008.1.11, which belonged to a *Mochlodon*-sized animal, renders it an unacceptable outlier in a single-species context even with the most extreme but still realistic degree of developmental plasticity (Ősi *et al*. 2012). Apart from this specimen, the only other adult *Rhabdodon* femur in the sample, MHN AIX PV 2007.4.116, shows strikingly different histology which may represent additional support for the distinct nature of MHN AIX PV 2008.1.11, although complete secondary remodelling in MHN AIX PV 2007.4.116 can simply reflect its senescence. Second, unlike all other *Rhabdodon* specimens that were found in the Vitrolles-Couperigne locality, MHN AIX PV 2008.1.11, along with some other, yet undescribed but also small appendicular elements was found 40 km away along the Jas Neuf Highway 3 or JNH3 (Tortosa *et al*. 2012). In addition, all undescribed elements found in JNH3 show mature morphologies in spite of being less than half the size of the large specimens known from the Vitrolles-Couperigne locality (Thierry Tortosa, pers. comm.). In any case, more complete specimens with diagnostic features are needed from this locality to decide whether differences are sufficient for a genus-level distinction of these rhabdodontids (this project is in progress led by T. Tortosa). Concerning the taxonomic composition of the rest of the investigated *Rhabdodon* specimens, there is not enough data to conclude either way. Based on the currently available data, it is very well possible that both developmental plasticity and heterogeneous species composition play a role in the detected variability in the histology-based ontogenetic pattern of *Rhabdodon*.

The power of histological features as potential taxonomic indicators is still dubious and certainly needs more investigation with numeric analysis of histomorphometric data. Although some osteohistological characters have been shown to have a weak phylogenetic signal (Cubo *et al*. 2005), it is to be expected that taxon-specificity in bone histology will not be detected at species level. Furthermore, bone being a highly adaptive, dynamic and responsive tissue (Currey, 2003), it is highly likely that most of the similarities are derived from common ecological factors (e.g., island-effect) influencing life history and functional aspects (body size, locomotor modes, etc.) rather than from constraints attributed to close phylogenetic relationships. Nonetheless, combined with available morphological, paleogeographical and geochronological data, histology is an essential tool in exploring taxonomic identities and phylogenetic patterns, and thereby inferring evolutionary pathways and processes that shape all varieties of traits.

ACKNOWLEDGEMENTS

I wish to thank Alexandra Houssaye and an anonymous reviewer for their critical comments and useful suggestions which improved the standards of the manuscript. Karl Rauscher (University of Vienna, Vienna, Austria), Patrick and Annie Mechin (Vitrolles, France); Gilles Cheylan, Yves Dutour and Thierry Tortosa (Natural History Museum, Aix-en-Provence, France) are thanked for access to material in their care, and Martin Sander for providing thin sections and partially technical background for my histological investigations. I am especially grateful to Thierry Tortosa for sharing his unpublished results. Special thanks go to Attila Ősi (MTA-ELTE Lendület Dinosaur Research Group) who provided specimens, useful comments, and a tremendous amount of motivation and support for this work. Koen Stein (Earth System Sciences, Vrije Universiteit Brussel, Brussels, Belgium) is acknowledged for fruitful discussions and for providing literature essential to this study. I thank Zsófia Hajdu, Réka Kalmár (MTA-ELTE Lendület Dinosaur Research Group), and Olaf Dülfer (IPB) for their technical assistance. Logistic background was provided by MTA–ELTE Lendület Program (Nr. 95102), Eötvös Loránd University, Department of Physical and Applied Geology, and the Hungarian Natural History Museum.

BIBLIOGRAPHY

Allain, R., Pereda-Suberbiola, X., 2003. Dinosaurs of France. Comptes Rendus Palevol 2, 27-44.

Amling, M., Takeda, S., Karsenty, G., 2000. A neuro (endo)crine regulation of bone remodeling. BioEssays 22, 970-975.

Ascenzi, A., Bonucci, E., 1967. The tensile properties of single osteons. The Anatomical Record 158, 375-386.

Ascenzi, A., Bonucci, E., 1968. The compressive properties of single osteons. The Anatomical Record 158, 375-386.

Benton, M. J., Csiki, Z., Grigorescu, D., Redelstorff, R., Sander, P. M., Stein, K., Weishampel, D. B., 2010. Dinosaurs and the island rule: The dwarfed dinosaurs from Haţeg Island. Palaeogeography, Palaeoclimatology, Palaeoecology 293, 438-454.

Björndal, K., Bolten, A. B., Bennett, R. A., Jacobson, E. R., Wronski, T. J., Valeski, J. J., Elizar, P. J., 1998. Age and growth in sea turtles: limitations of skeletochronology for demographic studies. Copeia 1, 23-30.

Buffetaut, E., Cuny, G., Le Loeuff, J., 1993. The discovery of French dinosaurs. Modern Geology 18, 161-182.

Buffrénil, V. d., Castanet, J., 2000. Age estimation by skeletochronology in the Nile monitor (*Varanus niloticus*), a highly exploited species. Journal of Herpetology 34, 414-424.

Buffrénil, V. d., Houssaye, A., Böhme, W., 2008. Bone vascular supply in Monitor lizards (Squamata: Varanidae): influence of size, growth, and phylogeny. Journal of Morphology 269, 533-543.

Bunzel, E., 1871. Die Reptilfauna der Gosau-Formation in der Neuen Welt bei Wiener-Neustadt. Abhandlungen der Kaiserlich-Königlichen geologischen Reichsanstalt 5, 1-18.

Castanet, J., Francillon-Vieillot, H., Meunier F., Ricqlès A. d., 1993. Bone and individual aging. In: Hall, B. K. (Ed.), Bones 7: Bone Growth. CRC Press, Ann Arbor, Michigan, pp. 245-283.

Chinsamy, A., 1993. Bone histology and growth trajectory of the prosauropod dinosaur *Massospondylus carinatus* Owen. Modern Geology 18, 319-329.

Chinsamy, A., 1995. Ontogenetic changes in the bone histology of the Late Jurassic ornithopod *Dryosaurus lettowvorbecki*. Journal of Vertebrate Paleontology 15(1), 96-104.

Chinsamy, A., Rich, T., Vickers-Rich, P., 1998. Polar dinosaur bone histology. Journal of Vertebrate Paleontology 18(2), 385-390.

Chinsamy-Turan, A., 2005. The microstructure of dinosaur bone: deciphering biology with fine-scale techniques. Johns Hopkins University Press, Baltimore.

Company, J., 2004. Vertebrados continentales del Cretácico Superior (Campaniense–Maastrichtiense) de València. PhD, Universitat de València.

Cormack, D. H., 1987. Ham's histology. Lippincott William and Wilkins, New York.

Crockett, J., Rogers, M. J., Coxon, F. P., Hocking, L. J., Helfrich, M. H., 2011. Bone remodelling at a glance. Journal of Cell Science 124, 991-998.

Cubo, J., Ponton, F., Laurin, M., Margerie, E. d., Castanet, J., 2005. Phylogenetic signal in bone microstructure of sauropsids. Systematic Biology 54(4), 562-574.

Currey, J. D., 2003. The many adaptations of bone. Journal of Biomechanics 36, 1487-1495.

Curry, K. A., 1999. Ontogenetic histology of *Apatosaurus* (Dinosauria: Sauropoda): New insights on growth rates and longevity. Journal of Vertebrate Paleontology 19(4), 654-665.

Enlow, D. H., 1962. A Study of the post-natal growth and remodeling of bone. American Journal of Anatomy 110(2), 79-101.

Erickson, G. M., 2005. Assessing dinosaur growth patterns: a microscopic revolution. Trends in Ecology and Evolution 20, 677-684.

Erickson, G. M., Tumanova, T. A., 2000. Growth curve of *Psittacosaurus mongoliensis* Osborn (Ceratopsia: Psittacosauridae) inferred from long bone histology. Zoological Journal of the Linnean Society 130, 551-566.

Erickson, G. M., Curry Rogers, K., Varricchio, D. J., Norell, M. A., Xu, X., 2007. Growth patterns in brooding dinosaurs reveal the timing of sexual maturity in non-avian dinosaurs and genesis of the avian condition. Biology Letters 3, 558-561.

Erickson, G. M., Rauhut, O. W. M., Zhou, Z., Turner, A. H., Inouye1, B. D., Hu, D., Norell, M. A., 2009. Was dinosaurian physiology inherited by birds? Reconciling slow growth in *Archaeopteryx*. PLoS ONE, 4(10), e7390, 1-9.

Esteban, M., García-París, M., Castanet, J., 1996. Use of bone histology in estimating the age of frogs (*Rana perezi*) from a warm temperate climate area. Canadian Journal of Zoology 74(10), 1914-1921.

Francillon-Vieillot, H., Buffrénil, V. D., Castanet, J., Géraudie, J., Meunier, F. J., Sire, J. Y., Zylberberg, L., Ricqlès, A. d. 1990. Microstructure and mineralization of vertebrate skeletal tissues. In: Carter, J.G. (Ed.), Skeletal Biomineralization: Patterns, Processes and Evolutionary Trends. Van Nostrand Reinhold, New York, pp. 471-530.

Frost, H. M., 1969. Tetracycline-based histological analysis of bone remodeling. Calcified Tissue Research 3, 211-237.

Godefroit, P., Codrea, V., Weishampel, D. B., 2009. Osteology of *Zalmoxes shqiperorum* (Dinosauria, Ornithopoda), based on new specimens from the Upper Cretaceous of Nalat¸-Vad (Romania). Geodiversitas 31(3), 525-553.

Green, W. C. H., Rothstein, A., 1991. Trade-offs between growth and reproduction in female bison. Oecologia 86(4), 521-527

Haines, W. R., 1942. The evolution of epiphyses and of endochondral bone. Biological Reviews 17(4), 267-292.

Horner, J. R., Ricqlès, A. d., Padian, K., 1999. Variation in dinosaur skeletochronology indicators: implications for age assessment and physiology. Paleobiology 25(3), 295-304.

Horner, J. R., Ricqlès, A. d., Padian, K., 2000. Long bone histology of the hadrosaurid dinosaur *Maiasaura peeblesorum*: growth dynamics and physiology based on an ontogenetic series of skeletal elements. Journal of Vertebrate Paleontology 20, 115-129.

Horner, J. R., Ricqlès, A. d., Padian, K., Scheetz, R. D., 2009. Comparative long bone histology and growth of the ''hypsilophodontid'' dinosaurs *Orodromeus makelai*, *Dryosaurus altus*, and *Tenontosaurus tillettii* (Ornithischia: Euornithopoda). Journal of Vertebrate Paleontology 29, 734-747.

Hübner, T. R., 2012. Bone histology in *Dysalotosaurus lettowvorbecki* (Ornithischia, Iguanodontia)—variation, growth, and implications. PLoS ONE 7(1), e29958, 1-29.

Jakob, C., Seitz, A., Crivelli A. J., Miaud, C., 2002. Growth cycle

of the marbled newt (*Triturus marmoratus*) in the Mediterranean region assessed by skeletochronology. Amphibia-Reptilia 23(4), 407-418.

Javed, A., Chen, H., Ghori, F. Y., 2010. Genetic and transcriptional control of bone formation. Oral and Maxillofacial Surgery Clinics of North America 22(3), 283-293.

Klein, N., Sander, M., 2008. Ontogenetic stages in the long bone histology of sauropod dinosaurs. Paleobiology 34, 248-264.

Klein, N., Scheyer, T., Tütken, T., 2009. Skeletochronology and isotopic analysis of a captive individual of *Alligator mississippiensis* Daudin, 1802. Fossil Record 12(2), 121-131.

Köhler, M., Marín-Moratalla, N., Jordana, X., Aanes, R., 2012. Seasonal bone growth and physiology in endotherms shed light on dinosaur physiology. Nature 487, 358-361.

Lee, A. H., Werning, S., 2008. Sexual maturity in growing dinosaurs does not fit reptilian growth models. Proceedings of the National Academy of Sciences USA 105, 582-587.

Marotti, G., 2010. Static and dynamic osteogenesis. Italian Journal of Anatomy and Embryology 115, 123-126.

Matheron, P., 1869. Notice sur les reptiles fossiles des dépôts fluvio-lacustres crétacés du bassin à lignite de Fuveau. Extraits des Mémoires de l'Academie Impériale des Sciences, Belles-Lettres et Arts de Marseilles 1869, 345-379.

Matsuki, T., Matsui, M., 2009. The validity of skeletochronology in estimating ages of Japanese Clouded Salamander, *Hynobius nebulosus* (Amphibia, Caudata). Current Herpetology 28(2), 41-48.

McDonald, A. T., 2012. Phylogeny of basal iguanodonts (Dinosauria: Ornithischia): An update.

Nopcsa, F., 1902. Dinosaurierreste aus Siebenbürgen II. (Schädelreste von *Mochlodon*). Mit einem Anhange: zur Phylogenie der Ornithopodiden. Denkschriften der Kaiserlichen Akademie der Wissenschaften Wien 72, 149-175.

Ősi, A., Prondvai, E., Butler, R., Weishampel, D. B., 2012. Phylogeny, histology and inferred body size evolution in a new rhabdodontid dinosaur from the Late Cretaceous of Hungary. PLoS ONE 7(9), e44318.

Pereda-Suberbiola, X., Sanz, J. L., 1999. The ornithopod dinosaur *Rhabdodon* from the Upper Cretaceous of Lan˜o (Iberian Peninsula). Estudios del Museo de Ciencias Naturales de Alava 14: 257-272.

Pogoda, P., Priemel, M., Rueger J. M., Amling, M., 2005. Bone remodeling: new aspects of a key process that controls skeletal maintenance and repair. Osteoporosis International 16, S18-S24.

Prondvai, E., Bodor, E. R., Ősi, A., 2014(b). Does morphology reflect osteohistology-based ontogeny? A case study of Late Cretaceous pterosaur jaw symphyses from Hungary reveals hidden taxonomic diversity. Paleobiology 40(2), 288-321.

Prondvai, E., Stein, K. H. W., Ricqlès, A. d., Cubo, J., 2014(a). Development-based revision of bone tissue classification: the importance of semantics for science. Biological Journal of the Linnean Society 112, 799-816.

Reiss, M. J., 1989. The Allometry of Growth and Reproduction. Cambridge University Press, New York.

Ricqlès, A. d., 1975. Recherches paléohistologiques sur les os longs des tétrapodes VII — Sur la classification, la signification fonctionelle et l'histoire des tissus osseux des tétrapodes. Première partie. Annales de Paléontologie 61, 51-129.

Sander, P.M., 2000. Long bone histology of the Tendaguru sauropods: implications for growth and biology. Paleobiology 26, 466-488.

Schmalhausen, I. I., 1949. Factors of evolution. University of Chicago Press, Chicago.

Seeley, H. G., 1881. The reptile fauna of the Gosau Formation preserved in the Geological Museum of the University of Vienna. With a note on the geological horizon of the fossils at Neue Welt, east of Wiener Neustadt. Quarterly Journal of the Geological Society, London 37, 620–707.

Smith, K. K., 2001. Heterochrony revisited: the evolution of developmental sequences. Biological Journal of the Linnean Society 73, 169-186.

Stein, K., Prondvai, E., 2014. Rethinking the nature of fibrolamellar bone: an integrative biological revision of sauropod plexiform bone formation. Biological Reviews 89, 24-47.

Stein, K., Csiki, Z., Curry Rogers, K., Weishampel, D. B., Redelstorff, R., Sander, P. M., 2010. Small body size and extreme cortical bone remodeling indicate phyletic dwarfism in *Magyarosaurus dacus* (Sauropoda: Titanosauria). Proceedings of the National Academy of Sciences, USA 107, 9258-9263.

Tortosa, T., Dutour, Y., Cheylan, G., Buffetaut, E., 2012. New discovery of titanosaurs (Dinosauria: Sauropoda) from Provence (SE France): implications on local paleobiodiversity. In: Royo-Torres, R., Gascó, F., Alcalá, L. (coord.), 10th Annual Meeting of the European Association of Vertebrate Palaeontologists. *¡Fundamental!* 20, 259-262.

Varricchio, D. J., 1993. Bone microstructure of the Upper Cretaceous theropod dinosaur *Troodon formosus*. Journal of Vertebrate Paleontology 13, 99-104.

Weishampel, D. B., Jianu, C. M., Csiki, Z., Norman, D. B., 2003. Osteology and phylogeny of *Zalmoxes* (n. g.), an unusual euornithopod dinosaur from the latest Cretaceous of Romania. Journal of Systematic Palaeontology 1, 65-123.

Wells, N. A., 1989. Making thin sections. In: Feldmann, R. M., Chapman, R. E., Hannibal J. T. (Eds.), Paleotechniques. University of Tennessee, Knoxville, pp. 120-129.

Werning, S., 2012. The ontogenetic osteohistology of *Tenontosaurus tilletti*. PLoS ONE 7(3), e33539.

Woodward, H. N., Rich, T. H., Chinsamy, A., Vickers-Rich, P., 2011. Growth dynamics of Australia's polar dinosaurs. PLoS ONE 6(8), e23339.